## REFERENCES


Akagi, K., Hirose, M., Hoshiya, T., Mizoguchi, Y., Ito, N., and Shirai, T. (1995). Modulating effects of ellagic acid, vanillin and quercetin in a rat medium term multi-organ carcinogenesis model. *Cancer Lett* **94**, 113-21.

Ashby, J., and Tennant, R. W. (1991). Definitive relationships among chemical structure, carcinogenicity and mutagenicity for 301 chemicals tested by the U.S. NTP. *Mutat Res* **257**, 229-306.

Bannasch, P. (1986). Preneoplastic lesions as end points in carcinogenicity testing. I. Hepatic preneoplasia. *Carcinogenesis* **7**, 689-95.

Cooper, J. A., 2nd, Saracci, R., and Cole, P. (1979). Describing the validity of carcinogen screening tests. *Br J Cancer* **39**, 87-9.

Fukushima, S., Hagiwara, A., Hirose, M., Yamaguchi, S., Tiwawech, D., and Ito, N. (1991). Modifying effects of various chemicals on preneoplastic and neoplastic lesion development in a wide-spectrum organ carcinogenesis model using F344 rats. *Jpn J Cancer Res* **82**, 642-9.

Hagiwara, A., Tanaka, H., Imaida, K., Tamano, S., Fukushima, S., and Ito, N. (1993). Correlation between medium-term multi-organ carcinogenesis bioassay data and long-term observation results in rats. *Jpn J Cancer Res* **84**, 237-45.

Hasegawa, R., and Ito, N. (1992). Liver medium-term bioassay in rats for screening of carcinogens and modifying factors in hepatocarcinogenesis. *Food Chem Toxicol* **30**, 979-92.

Higginson, G., and Anderson, R. (1931). Experimental pathology of the liver. 1. Restoration of the liver of the white rat following partial surgical removal. *Arch Pathol* **12**, 186–202.

ICH Steering Committee, I. (1997). International Conference on Harmonization: Carcinogenicity: testing for carcinogenicity of pharmaceuticals. In Proceedings of Fourth International Conference on Harmonization..

Ito, N., Hasegawa, R., Imaida, K., Hirose, M., and Shirai, T. (1996). Medium-term liver and multi-organ carcinogenesis bioassays for carcinogens and chemopreventive agents. *Exp Toxicol Pathol* **48**, 113-9.

Ito, N., Hasegawa, R., Imaida, K., Hirose, M., Shirai, T., Tamano, S., and Hagiwara, A. (1997). Medium-term rat liver bioassay for rapid detection of hepatocarcinogenic substances. *J Toxicol Pathol* 1–11.

Ito, N., Hasegawa, R., Imaida, K., Masui, T., Takahashi, S., and Shirai, T. (1992). Pathological markers for non-genotoxic agent-associated carcinogenesis. *Toxicol Lett* **64**, 613-20.

Ito, N., Tamano, S., and Shirai, T. (2003). A medium-term rat liver bioassay for rapid in vivo detection of carcinogenic potential of chemicals. *Cancer Sci* **94**, 3-8.

Kitahara, A., Satoh, K., Nishimura, K., Ishikawa, T., Ruike, K., Sato, K., Tsuda, H., and Ito, N. (1984). Changes in molecular forms of rat hepatic glutathione S-transferase during chemical hepatocarcinogenesis. *Cancer Res* **44**, 2698-703.

Liu, L. L., Gong, L. K., Qi, X. M., Cai, Y., Wang, H., Wu, X. F., Xiao, Y., and Ren, J. (2005). Altered expression of cytochrome P450 and possible correlation with preneoplastic changes in early stage of rat hepatocarcinogenesis. *Acta Pharmacol Sin* **26**, 737-44.

Matsumoto, K., and Nakamura, T. (1992). Hepatocyte growth factor: molecular structure, roles in liver regeneration, and other biological functions. *Crit Rev Oncog* **3**, 27-54.

Oesterle, D., and Deml, E. (1990). Detection of chemical carcinogens by means of the "rat liver foci bioassay." *Exp Pathol* **39**, 197-206.

Ogawa, K., Yokokawa, K., Tomoyori, T., and Onoe, T. (1982). Induction of gamma-glutamyltranspeptidase-positive altered hepatocytic lesions by combination of transplacental-initiation and postanal-selection. *Int J Cancer* **29**, 333-6.

Ogiso, T., Tatematsu, M., Tamano, S., Tsuda, H., and Ito, N. (1985). Comparative effects of carcinogens on the induction of placental glutathione S-transferase-positive liver nodules in a short-term assay and of hepatocellular carcinomas in a long-term assay. *Toxicol Pathol* **13**, 257-65.

Peraino, C., Fry, R. J., Staffeldt, E., and Christopher, J. P. (1975). Comparative enhancing effects of phenobarbital, amobarbital, diphenylhydantoin, and dichlorodiphenyltrichloroethane on 2-acetylaminofluorene-induced hepatic tumorigenesis in the rat. *Cancer Res* **35**, 2884-90.

Peraino, C., Fry, R. J., Staffeldt, E., and Christopher, J. P. (1977). Enhancing effects of phenobarbitone and butylated hydroxytoluene on 2-acetylaminofluorene-induced hepatic tumorigenesis in the rat. *Food Cosmet Toxicol* **15**, 93-6.

Peraino, C., Staffeldt, E. F., Haugen, D. A., Lombard, L. S., Stevens, F. J., and Fry, R. J. (1980). Effects of varying the dietary concentration of phenobarbital on its enhancement of 2-acetylaminofluorene-induced hepatic tumorigenesis. *Cancer Res* **40**, 3268-73.

Pitot, H., and Dragan, Y. (2001). Chemical carcinogenesis. In Casertt & Doul's TOXICOLOGY: The basic science of poisons, 6th ed. (I. K. CD, ed.), pp. 241–319. McGraw-Hill, New York.

Shirai, T. (1997). A medium-term rat liver bioassay as a rapid in vivo test for carcinogenic potential: a historical review of model development and summary of results from 291 tests. *Toxicol Pathol* **25**, 453-60.

Shirai, T., Hirose, M., and Ito, N. (1999). The use of short-and medium-term tests for carcinogens and data on genetic effects in carcinogenic hazard evaluation. Consensus report. In IARC Sci Publ, pp. 1-18..

Solt, D., and Farber, E. (1976). New principle for the analysis of chemical carcinogenesis. *Nature* **263**, 701–3.

Tatematsu, M., Mera, Y., Ito, N., Satoh, K., and Sato, K. (1985). Relative merits of immunohistochemical demonstrations of placental, A, B and C forms of glutathione S-transferase and histochemical demonstration of gamma-glutamyl transferase as markers of altered foci during liver carcinogenesis in rats. *Carcinogenesis* **6**, 1621-6.

Tatematsu, M., Shirai, T., Tsuda, H., Miyata, Y., Shinohara, Y., and Ito, N. (1977). Rapid production of hyperplastic liver nodules in rats treated with carcinogenic chemicals: a new approach for an in vivo short-term screening test for hepatocarcinogens. *Gann* **68**, 499-507.

Tsuda, H., Asamoto, M., Iwahori, Y., Hori, T., Ota, T., Baba-Toriyama, H., Uehara, N., Kim, D. J., Krutovskikh, V. A., Takasuka, N., et al. (1996). Decreased connexin32 and a characteristic enzyme phenotype in clofibrate-induced preneoplastic lesions not shared with spontaneously occurring lesions in the rat liver. *Carcinogenesis* **17**, 2441-8.

Tsuda, H., Fukushima, S., Wanibuchi, H., Morimura, K., Nakae, D., Imaida, K., Tatematsu, M., Hirose, M., Wakabayashi, K., and Moore, M. A. (2003). Value of GST-P positive preneoplastic hepatic foci in dose-response studies of hepatocarcinogenesis: evidence for practical thresholds with both genotoxic and nongenotoxic carcinogens. A review of recent work. *Toxicol Pathol* **31**, 80-6.

Tsuda, H., Hasegawa, R., Imaida, K., Masui, T., Moore, M. A., and Ito, N. (1984). Modifying potential of thirty-one chemicals on the short-term development of gamma-glutamyl transpeptidase-positive foci in diethylnitrosamine-initiated rat liver. *Gann* **75**, 876-83.

Tsuda, H., Lee, G., and Farber, E. (1980). Induction of resistant hepatocytes as a new principle for a possible short-term in vivo test for carcinogens. *Cancer Res* **40**, 1157-64.

Tsuda, H., Moore, M. A., Asamoto, M., Inoue, T., Ito, N., Satoh, K., Ichihara, A., Nakamura, T., Amelizad, Z., and Oesch, F. (1988). Effect of modifying agents on the phenotypic expression of cytochrome P-450, glutathione S-transferase molecular forms, microsomal epoxide hydrolase, glucose-6-phosphate dehydrogenase and gamma-glutamyltranspeptidase in rat liver preneoplastic lesions. *Carcinogenesis* **9**, 547-54.

Tsuda, H., Moore, M. A., Asamoto, M., Satoh, K., Tsuchida, S., Sato, K., Ichihara, A., and Ito, N. (1985). Comparison of the various forms of glutathione S-transferase with glucose-6-phosphate dehydrogenase and gamma-glutamyltranspeptidase as markers of preneoplastic and neoplastic lesions in rat kidney induced by N-ethyl-N-hydroxyethylnitrosamine. *Jpn J Cancer Res* **76**, 919-29.

Tsuda, H., Ozaki, K., Uwagawa, S., Yamaguchi, S., Hakoi, K., Aoki, T., Kato, T., Sato, K., and Ito, N. (1992). Effects of modifying agents on conformity of enzyme phenotype and proliferative potential in focal preneoplastic and neoplastic liver cell lesions in rats. *Jpn J Cancer Res* **83**, 1154-65.

Ward, J. M., Tsuda, H., Tatematsu, M., Hagiwara, A., and Ito, N. (1989). Hepatotoxicity of agents that enhance formation of focal hepatocellular proliferative lesions (putative preneoplastic foci) in a rapid rat liver bioassay. *Fundam Appl Toxicol* **12**, 163-71.

**Carcinogenesis** vol.31 no.5 pp.927–935, 2010
doi:10.1093/carcin/bgq029
*Advance Access publication February 25, 2010*

# Involvement of macrophage inflammatory protein 1α (MIP1α) in promotion of rat lung and mammary carcinogenic activity of nanoscale titanium dioxide particles administered by intra-pulmonary spraying

**Jiegou Xu[1], Mitsuru Futakuchi[1], Masaaki Iigo[1], Katsumi Fukamachi[1], David B.Alexander[1], Hideo Shimizu[2], Yuto Sakai[1,3], Seiko Tamano[4], Fumio Furukawa[4], Tadashi Uchino[5], Hiroshi Tokunaga[6], Tetsuji Nishimura[5], Akihiko Hirose[5], Jun Kanno[5] and Hiroyuki Tsuda[1,*]**

[1]Department of Molecular Toxicology and [2]Core Laboratory, Nagoya City University Graduate School of Medical Sciences, 1-Kawasumi, Mizuho-cho, Mizuho-ku, Nagoya 467-8601, Japan, [3]Department of Drug Metabolism and Disposition, Graduate School of Pharmaceutical Sciences, 3-1, Tanabe-Dohri, Mizuho-ku, Nagoya 467-8603, Japan, [4]DIMS Institute of Medical Science, Inc., 64 Goura, Nishiazai, Azai-cho, Ichinomiya 491-0113, Japan, [5]National Institute of Health Sciences, 1-18-1 Kamiyoga, Setagaya-ku, Tokyo 158-8501, Japan and [6]Pharmaceuticals and Medical Devices Agency, 2-3-3, Kasumigaseki, Chiyoda-ku, Tokyo 100-0013, Japan

*To whom correspondence should be addressed. Tel: +81 52 853 8991; Fax: +81 52 853 8996;
Email: htsuda@med.nagoya-cu.ac.jp

**Titanium dioxide ($TiO_2$) is evaluated by World Health Organization/International Agency for Research on Cancer as a Group 2B carcinogen. The present study was conducted to detect carcinogenic activity of nanoscale $TiO_2$ administered by a novel intrapulmonary spraying (IPS)-initiation–promotion protocol in the rat lung. Female human c-Ha-*ras* proto-oncogene transgenic rat (H*ras*128) transgenic rats were treated first with *N*-nitrosobis(2-hydroxypropyl)amine (DHPN) in the drinking water and then with $TiO_2$ (rutile type, mean diameter 20 nm, without coating) by IPS. $TiO_2$ treatment significantly increased the multiplicity of DHPN-induced alveolar cell hyperplasias and adenomas in the lung, and the multiplicity of mammary adenocarcinomas, confirming the effectiveness of the IPS-initiation–promotion protocol. $TiO_2$ aggregates were localized exclusively in alveolar macrophages and had a mean diameter of 107.4 nm. To investigate the underlying mechanism of its carcinogenic effects, $TiO_2$ was administered to wild-type rats by IPS five times over 9 days. $TiO_2$ treatment significantly increased 8-hydroxydeoxy guanosine level, superoxide dismutase activity and macrophage inflammatory protein 1α (MIP1α) expression in the lung. MIP1α, detected in the cytoplasm of $TiO_2$-laden alveolar macrophages *in vivo* and in the media of rat primary alveolar macrophages treated with $TiO_2$ *in vitro*, enhanced proliferation of human lung cancer cells. Furthermore, MIP1α, also detected in the sera and mammary adenocarcinomas of $TiO_2$-treated H*ras*128 rats, enhanced proliferation of rat mammary carcinoma cells. These data indicate that secreted MIP1α from $TiO_2$-laden alveolar macrophages can cause cell proliferation in the alveoli and mammary gland and suggest that $TiO_2$ tumor promotion is mediated by MIP1α acting locally in the alveoli and distantly in the mammary gland after transport via the circulation.**

## Introduction

Inhalation of particles and fiber is well known to be strongly associated with increased lung cancer risk in the workplace (1,2). Although the size of fiber particles was reported to be closely related to risk (3), the precise role of particles and fibers in lung cancer induction has not yet been elucidated.

Titanium dioxide ($TiO_2$) particles of various sizes are manufactured worldwide in large quantities and are used in a wide range of applications. $TiO_2$ particles have long been considered to pose little risk to respiratory health because they are chemically and thermally stable. However, $TiO_2$ is classified as a Group 2B carcinogen, a possible carcinogen to humans, by World Health Organization/International Agency for Research on Cancer based on the findings of lung tumor induction in female rats (3,4). This overall evaluation includes nanoscale (<100 nm in diameter) and larger sized classes of $TiO_2$. At present, the mechanism underlying the development of rat lung tumors by inhalation of $TiO_2$ particles is unclear.

Inhalation of $TiO_2$ particles can occur both at the workplace, e.g. in manufacturing and packing sites, and also outside the workplace during their use (5–7). Exposure to airborne nanoparticles has been reported to be associated with a granulomatous inflammatory response in the lung (8). Inhalation studies of nanoparticles for cancer risk assessment is urgently needed, however, due to the high cost of long-term studies, available data is severely limited (9,10). The aim of this study is to understand the mechanism underlying rat lung carcinogenesis induced by inhalation of $TiO_2$ particles. We choose intrapulmonary spraying (IPS) because it does not require costly facilities, allows accurate dose control and approximates long-term inhalation studies (3,11).

We initially examined whether $TiO_2$ particles have carcinogenic activity in the rat lung using a novel IPS-initiation–promotion protocol (12,13). For these experiments, Sprague–Dawley (SD)-derived female human c-Ha-*ras* proto-oncogene transgenic rat (H*ras*128) transgenic rats, which are known to have the same carcinogen susceptibility phenotype in the lung as wild-type rats but are highly susceptible to mammary tumor induction (14–16), were treated with *N*-nitrosobis(2-hydroxypropyl)amine (DHPN) to initiate carcinogenesis and then treated with $TiO_2$ by IPS. We observed a promotion effect of $TiO_2$ particles in lung and mammary gland carcinogenesis.

To identify factors involved in this promotion effect, wild-type SD strain rats were treated with $TiO_2$ by IPS for 9 days. We found macrophage inflammatory protein 1α (MIP1α) was produced by $TiO_2$-laden alveolar macrophages in the lungs of rats treated with $TiO_2$. MIP1α is a member of the CC chemokine family and is primarily associated with cell adhesion and migration of multiple myeloma cells (17). It is reported to be produced by macrophages in response to a variety of inflammatory stimuli including $TiO_2$ (18). In the present study, MIP1α, detected in the medium of rat primary alveolar macrophages treated with $TiO_2$, enhanced proliferation of human lung cancer cells *in vitro*. MIP1α was also detected in the sera and mammary adenocarcinomas of $TiO_2$-treated H*ras*128 rats and enhanced proliferation of rat mammary carcinoma cells.

## Materials and methods

### *Animals*

Female transgenic rats carrying the H*ras*128 and female wild-type SD rats were obtained from CLEA Japan Co., Ltd (Tokyo, Japan) (15). The animals were housed in the animal center of Nagoya City University Medical School, maintained on a 12 h light–dark cycle and received Oriental MF basal diet (Oriental Yeast Co., Tokyo, Japan) and water *ad libitum*. The research was conducted according to the Guidelines for the Care and Use of Laboratory Animals of

**Abbreviations:** CCR1, C-C chemokine receptor type 1; DHPN, *N*-nitrosobis (2-hydroxypropyl) amine; ERK, extracellular signal-regulated kinase; GRO, growth-regulated oncogene; H*ras*128 rat, human c-Ha-*ras* proto-oncogene transgenic rat; IL, interleukin; IPS, intrapulmonary spraying; MEK1, MAPK/ERK kinase1; MIP1α, macrophage inflammatory protein 1α; 8-OHdG, 8-hydroxydeoxy guanosine; PBS, phosphate-buffered saline; ROS, reactive oxygen species; SD, Sprague–Dawley; SOD, superoxide dismutase; TEM, transmission electron microscopy; $TiO_2$, titanium dioxide.

 

Nagoya City University Medical School and the experimental protocol was approved by the Institutional Animal Care and Use Committee (H17-28).

*Preparation of $TiO_2$ and IPS*

$TiO_2$ particles (rutile type, without coating; with a mean primary size of 20 nm) were provided by Japan Cosmetic Association, Tokyo, Japan. $TiO_2$ particles were suspended in saline at 250 μg/ml or 500 μg/ml. The suspension was autoclaved and then sonicated for 20 min just before use. The $TiO_2$ suspension was intratracheally administered to animals under isoflurane anesthesia using a Microsprayer (Series IA-1B Intratracheal Aerosolizer, Penn-Century, Philadelphia, PA) connected to a 1 ml syringe: the nozzle of the sprayer was inserted into the trachea through the larynx and a total of 0.5 ml suspension was sprayed into the lungs synchronizing with spontaneous respiratory inhalation (IPS).

*IPS-initiation–promotion protocol*

Thirty-three female H*ras*128 rats aged 6 weeks were given 0.2% DHPN, (Wako Chemicals Co., Ltd Osaka, Japan) in the drinking water for 2 weeks and 9 rats were given drinking water without DHPN. Two weeks later, the rats were divided into four groups, DHPN alone (Group 1), DHPN followed by 250 μg/ml $TiO_2$ (Group 2), DHPN followed by 500 μg/ml $TiO_2$ (Group 3) and 500 μg/ml $TiO_2$ without DHPN (Group 4). The $TiO_2$ particle preparations were administered by IPS once every 2 weeks from the end of week 4 to week 16 (a total of seven times). The total amount of $TiO_2$ administered to Groups 1, 2, 3 and 4 were 0, 0.875, 1.75 and 1.75 mg per rat, respectively. Three days after the last treatment, animals were killed and the organs (brain, lung, liver, spleen, kidney, mammary gland, ovaries, uterus and neck lymph nodes) were excised and divided into two pieces; one piece was immediately frozen at −80°C and used for quantitative measurement of elemental titanium, and the other piece was fixed in 4% paraformaldehyde solution in phosphate-buffered saline (PBS) buffer adjusted to pH 7.3 and processed for light microscopic examination and transmission electron microscopy (TEM); the left lungs and inguinal mammary glands were used for elemental titanium analysis and the right lungs and inguinal mammary glands were used for microscopic examination.

*IPS 9 day protocol*

Twenty female SD rats (wild-type counterpart of H*ras*128) aged 10 weeks were treated by IPS with 0.5 ml suspension of 500 μg/ml $TiO_2$ particles in saline five times over a 9 day period (Figure 2A). The total amount of $TiO_2$ administered was 1.25 mg per rat. Six hours after the last dose, animals were killed and the lungs and inguinal mammary glands were excised. Fatty tissue surrounding the mammary gland was removed as much as possible. The left lungs and inguinal mammary glands were used for biochemical analysis, and the right lungs were fixed in 4% paraformaldehyde solution in PBS adjusted at pH 7.3 and processed for histopathological examination and immunohistochemistry.

*Light microscopic and TEM observation of $TiO_2$ particles in the lung*

Paraffin blocks were deparaffinized and embedded in epon resin and processed for $TiO_2$ particle observation and titanium element analysis, using a JEM-1010 transmission electron microscope (JEOL Co. Ltd, Tokyo, Japan) equipped with an X-ray microanalyzer (EDAX, Tokyo, Japan). Size analysis of $TiO_2$ particles was performed using TEM photos by an image analyzer system, (IPAP, Sumika Technos Corporation, Osaka, Japan). A total of 452 particles from alveolar macrophages from rats in Group 3 (DHPN followed by 500 μg/ml $TiO_2$) of the IPS-initiation–promotion study and a total of 2571 particles from alveolar macrophages from rats in the IPS 9 day study were measured.

*Biochemical element analysis of titanium*

For the detection of elemental titanium, frozen tissue samples of 50–100 mg were digested with 5 ml concentrated $HNO_3$ for 22 min in a microwave oven. Titanium in the digested solutions was determined by inductively coupled plasma–mass spectrometry (HP-4500, Hewlett-Packard Co., Houston, TX) under the following conditions: RF power, 1450 W; RF refraction current, 5 W; Plasma gas current, 15 l/min; Carrier gas current, 0.91 l/min; Peri pump, 0.2 r.p.s.; Monitoring mass-m/z 48 (Ti); Integrating interval, 0.1 s; Sampling period 0.31 s.

*Analysis of superoxide dismutase activity, 8-hydroxydeoxy guanosine and cytokine levels*

For the analysis of superoxide dismutase (SOD) activity, 8-hydroxydeoxy guanosine (8-OHdG) and cytokine levels, animals exposed to $TiO_2$ particles for 9 days were used. For 8-OHdG levels, genomic DNA was isolated from the left lung and inguinal mammary gland with a DNA Extractor WB Kit (Wako Chemicals Co. Ltd). 8-OHdG levels were determined with an 8-OHdG ELISA Check Kit (Japan Institute for the Control of Aging, Shizuoka, Japan) and by a custom service (OHG Institute Co., Ltd, Fukuoka, Japan). For the analysis of SOD activity and inflammation-related cytokines, tissue from the left lung and inguinal mammary glands was excised and rinsed with cold PBS three times and homogenized in 1 ml of T-PER, Tissue Protein Extraction Reagent (Pierce, Rockford, IL), containing 1% (vol/vol) proteinase inhibitor cocktail (Sigma–Aldrich, St Louis, MO). The homogenates were clarified by centrifugation at 10 000*g* for 5 min at 4°C. Protein content was measured using a BCA™ Protein Assay Kit (Pierce). SOD activity was determined using an SOD Assay Kit (Cayman Chemical Co., Ann Arbor, MI). The levels of interleukin (IL)-1α, IL-1β, IL-6, granulocyte-macrophage colony-stimulating factor, granulocyte colony-stimulating factor, tumor necrosis factor α, interferon γ, IL-18, monocyte chemotactic protein 1 and MIP1α, growth-regulated oncogene (GRO) and vascular endothelial growth factor were measured by Multiplex Suspension array (GeneticLab Co., Ltd, Sapporo, Japan).

*Immunohistochemistry*

CD68 and MIP1α were detected using anti-rat CD68 (BMA Biomedicals, Augst, Switzerland) and anti-rat MIP1α polyclonal antibodies (BioVision, Lyon, France). Both antibodies were diluted 1:100 in blocking solution and applied to slides, and the slides were incubated at 4°C overnight. The slides were then incubated for 1 h with biotinylated species-specific secondary antibodies diluted 1:500 (Vector Laboratories, Burlingame, CA) and visualized using avidin-conjugated alkaline phosphatase complex (ABC kit, Vector Laboratories) and Alkaline Phosphatase Substrate Kit (Vector Laboratories).

*Isolation of primary alveolar macrophages and preparation of conditioned media*

Wild-type female SD rats were given 0.5 ml 6% thioglycollate medium (Thioglycollate Medium II, Eiken Chemical Co., Ltd, Tokyo, Japan) by IPS on days 1, 3 and 5, and 6 h after the last treatment, the lungs were excised and minced with sterilized scissors in RPMI 1640 containing 10% fetal bovine serum (Wako Chemicals Co., Ltd) and antibiotics. The homogenate was washed twice and plated onto 6 cm dishes and incubated for 2 h at 37°C, 5% $CO_2$. The dishes were then washed with PBS three times to remove unattached cells and cell debris. Samples of the remaining adherent cells were cultured in chamber slides and immunostained for CD68 to confirm their identity as macrophages; ~98% of the cells were positive for CD68.

Primary alveolar macrophages were treated with vehicle or $TiO_2$ particles in saline suspension at a final concentration of 100 μg/ml and then incubated for 24 h in a 37°C, 5% $CO_2$ incubator. The conditioned medium was collected and diluted 5-fold with RPMI 1640; the conditioned medium had a final concentration of 2% fetal bovine serum.

*Western blotting*

For the detection of MIP1α, aliquots of 20 μg protein from the extracts of lung or mammary tissue were separated by 15% sodium dodecyl sulfate–polyacrylamide gel electrophoresis, transferred to nitrocellulose membranes and immunoblotted. For the detection of C-C chemokine receptor type 1 (CCR1), 10% sodium dodecyl sulfate–polyacrylamide gel electrophoresis was used for the separation. Membranes were probed overnight at 4°C with anti-rat MIP1α polyclonal antibody (BioVision) diluted at 1:100 or anti-CCR1 (Santa Cruz Biotechnology, Santa Cruz, CA) diluted at 1:100. The blots were washed and incubated for 1 h with biotinylated anti-species-specific secondary antibodies (Amersham Biosciences, Piscataway, NJ) and then visualized using ECL Western Blotting Detection Reagent (Amersham Biosciences). To ensure equal protein loading, the blots were striped with Restore Western Blot Stripping Buffer (Pierce) and reprobed with anti-β actin antibody (dilution 1:2000; Sigma–Aldrich) for 1 h at room temperature.

For the detection of serum MIP1α, GRO and IL-6, aliquots of 150 μg of protein from the sera of rats treated with $TiO_2$ for 16 weeks were subjected to sodium dodecyl sulfate–polyacrylamide gel electrophoresis. Anti-human GRO polyclonal antibody (BioVision) and anti-mouse IL-6 polyclonal antibody (Santa Cruz) were diluted 1:100. For detection of activated extracellular signal-regulated kinase (ERK) 1/2 and total ERK1/2, phospho ERK1/2 antiboby (Cell signaling Technology, Beverly, MA) and ERK1/2 antibody (Upstate, Lake placid, NY) were diluted 1:2000 and 1:25 000, respectively. The conditioned medium from alveolar macrophages, prepared as described above, was also subjected to western blot assay for MIP1α detection as described above. The blots were striped with Restore Western Blot Stripping Buffer (Pierce) and stained with Ponceau S solution (Sigma–Aldrich) for 10 min. The major band at 66 kDa was judged to be albumin and used as an internal control.

*In vitro cell proliferation assay*

A549 cells, a human lung cancer cell line, and the rat mammary cancer cell line C3 (19), derived from the H*ras*128 transgenic rats, were used in the *in vitro* cell proliferation assays. A549 or C3 cells were seeded into 96-well culture plates at $5 \times 10^3$ cells per well in 2% fetal bovine serum Dulbecco's modified Eagle's medium (Wako Chemicals Co., Ltd). After overnight incubation, the cells were treated as noted below, incubated for 72 h and the relative cell number was then determined.

To investigate the effect of culture supernatant from alveolar macrophages on A549 cell proliferation, their media were replaced with diluted conditioned medium, and the cells were incubated for 72 h with 0, 5, 10 and 20 μg/ml of anti-MIP1α neutralizing antibody (R&D Systems, Minneapolis, MN) or with 20 μg/ml of irrelevant IgG. To investigate the effect of recombinant cytokines on A549 cell proliferation, 10, 50 or 100 ng/ml of recombinant protein, rat MIP1α (R&D Systems), human GRO (R&D Systems) or human IL-6 (R&D Systems), was added to A549 cells. To investigate the role of ERK in MIP1α-stimulated cell proliferation, A549 cells, treated with or without $2 \times 10^{-7}$ M of the specific MAPK/ERK kinase1 (MEK1) inhibitor PD98059 (Cell Signaling Technology) for 10 min, were treated with 50 ng/ml of MIP1α protein. To investigate the effect of reactive oxygen species (ROS) on cell proliferation, A549 cells, with or without pretreatment with 1 mM *N*-acetyl cysteine (Wako Chemicals Co. Ltd) for 30 min, were treated with 0.5 mM $H_2O_2$ (Wako Chemicals Co. Ltd). To investigate of the effects of MIP1α on rat mammary cells, C3 cells were treated with serially diluted recombinant rat MIP1α (0, 0.4, 2.0, 10 and 50 ng/ml, respectively; R&D Systems). For detecting the direct effect of $TiO_2$ particles on A549 and C3 cell proliferation, $5 \times 10^3$ A549 or C3 cells were cultured overnight and then treated with 10 or 50 μg/ml of $TiO_2$ particles.

After 72 h incubation, the relative cell number of A549 and C3 was determined using the Cell Counting Kit-8 (Dojindo Molecular Technologies, Rockville, MD) according to the manufacturer's instruction.

*Statistical analysis*

For *in vivo* data, statistical analysis was performed using the Kruskal–Wallis and Bonferroni–Dunn's multiple comparison tests. *In vitro* data are presented as means ± standard deviations. The statistical significance of *in vitro* findings was analyzed using a two-tailed Student's *t*-test and Bonferroni–Dunn's multiple comparison tests. A value of $P < 0.05$ was considered significant. The Spearman's rank correlation test was used to determine the association between $TiO_2$ dose and $TiO_2$ carcinogenic activity.

## Results

*Promoting effects of $TiO_2$ particles in DHPN-induced lung and mammary carcinogenesis*

Prior to initiation of the IPS-initiation–promotion and IPS 9 day studies, we conducted a preliminary study to confirm whether IPS would be a good tool to deliver $TiO_2$ particles to the alveoli. Rats were treated by IPS with India ink. We observed that ink particles of ~50 to 500 μm in diameter were diffusely distributed throughout the alveoli space (data not shown), confirming that IPS could deliver $TiO_2$ particles to the alveoli.

Four groups of female H*ras*128 rats were treated with +/− DHPN to initiate carcinogenesis and then treated with $TiO_2$ by IPS for 12 weeks: Group 1, DHPN alone; Group 2, DHPN followed by 250 μg/ml $TiO_2$; Group 3, DHPN followed by 500 μg/ml $TiO_2$ and Group 4, 500 μg/ml $TiO_2$ without DHPN. Microscopic observation in the lung showed scattered inflammatory foci, alveolar cell hyperplasia (Figure 1A) and adenomas in the DHPN-treated rats. The multiplicity (numbers per square centimeter lung) of hyperplasias and adenomas in Group 3 (DHPN followed by 500 μg/ml $TiO_2$) were significantly increased compared with Group 1 (DHPN followed by saline, Table I), and the increase showed a dose-dependent correlation (rho = 0.630, $P = 0.001$ for hyperplasias and rho = 0.592, $P = 0.029$ for adenomas) by the Spearman's rank correlation test. In the mammary gland, $TiO_2$ treatment significantly increased the multiplicity of adenocarcinomas (Figure 1C) and tended to increase the weight of the mammary tumors (Figure 1C). In the rats, which received $TiO_2$ treatment without prior DHPN treatment, alveolar proliferative lesions were not observed although slight inflammatory lesions were observed.

$TiO_2$ was distributed primarily to the lung, but minor amounts of $TiO_2$ were also found in other organs (supplementary Figure 1A is available at *Carcinogenesis* Online).

Various sizes of $TiO_2$ aggregates were observed in alveolar macrophages (Figure 1B). The $TiO_2$-laden macrophages were evenly scattered throughout the lung alveoli. The number of hyperplasias with $TiO_2$-laden macrophages was dose dependently increased (supplementary Table 1 is available at *Carcinogenesis* Online). This result suggests that $TiO_2$-laden macrophages may be involved in the promotion of alveolar hyperplasia.

The size distribution of $TiO_2$ particle aggregate is shown in Figure 1D. Of 452 particle aggregates examined, 362 (80.1%) were nanosize, i.e. <100 nm. Overall, the average size was 84.9 nm and the median size was 44.4 nm.

*IPS 9 day study—analysis of $TiO_2$*

Female SD rats were treated with $TiO_2$ by IPS over a 9 day period (Figure 2A). Microscopic observation showed scattered inflammatory lesions with infiltration of numerous macrophages mixed with a few neutrophils and lymphocytes in $TiO_2$-treated animals. Overall, the number of macrophages in the alveoli was significantly increased in the $TiO_2$-treated animals (Figure 2B). As expected from the results of the IPS-initiation–promotion study, alveolar proliferative lesions were not observed (Figure 2C).

Morphologically, $TiO_2$ particles were observed as yellowish, polygonal bodies in the cytoplasm of cells (Figure 2D). These cells are morphologically distinct from neutrophils and strongly positive for CD68 (Figure 2E), indicating that the $TiO_2$ engulfing cells were macrophages. $TiO_2$ aggregates of various sizes were found in macrophages, and aggregates larger than a single macrophage were surrounded by multiple macrophages (supplementary Figure 1B is available at *Carcinogenesis* Online)

TEM also showed electron dense bodies in the cytoplasm of macrophages (Figure 2F and G). These bodies were found exclusively in macrophages and not found in the alveolar parenchyma, including alveolar epithelium and alveolar wall cells, or in any other cell type. The shape of the electron dense $TiO_2$ particles in the cytoplasm was quite similar to that observed in preparations taken from $TiO_2$ suspensions before administration (Figure 2H and supplementary Figure 1C and D is available at *Carcinogenesis* Online). Individual $TiO_2$ particles were rod-like in shape (supplementary Figure 1C is available at *Carcinogenesis* Online).

Element analysis by TEM and X-ray microanalysis indicated that these electron dense bodies were composed primarily of titanium particles (supplementary Figure 1E and F-1 and 1F-2 is available at *Carcinogenesis* Online). Titanium was not observed in the surrounding alveolar cells without electron dense bodies (supplementary Figure 1F-3 is available at *Carcinogenesis* Online). The size distribution of $TiO_2$ particle aggregates is shown in Figure 2I. Of 2571 particle aggregates examined, 1970 (76.6%) were <100 nm and five particles were >4000 nm in size. Overall, the average size was 107.4 nm and the median size was 48.1 nm.

*IPS 9 day study—analysis of oxidative stress and inflammation-related factors in the lungs of wild-type rats*

IPS of $TiO_2$ particles significantly increased SOD activity (Figure 3A) and 8-OHdG levels (Figure 3B) in the lungs of wild-type rats, but not in the mammary glands. Analysis of the expression levels of 12 cytokines using suspension array indicated that administration of $TiO_2$ particles significantly upregulated the expression of MIP1α, GRO and IL-6 in the lung tissue of wild-type rats (supplementary Table 2 is available at *Carcinogenesis* Online). MIP1α levels were slightly elevated (0.4 pg/mg protein) in the mammary gland (Figure 3C), although the elevation was not statistically significant. Elevation of MIP1α in the lung tissue of animals treated with $TiO_2$ particles was confirmed by western blotting (Figure 3D).

Immunohistochemically, MIP1α was detected in the cytoplasm of alveolar macrophages with phagocytosed $TiO_2$ particles (Figure 3E upper, stained in red) and these macrophages could be found in hyperplastic lesions of the lung (supplementary Figure 2A and B is available at *Carcinogenesis* Online). MIP1α was not detected in macrophages without $TiO_2$ particles (Figure 3E lower). Expression of CCR1, the major receptor of MIP1α, was observed in the lung; IPS of $TiO_2$ particles had little or no effect on CCR1 expression (supplementary Figure 2C is available at *Carcinogenesis* Online).

*Effect of MIP1α on proliferation of a human lung cancer cell line in vitro*

Alveolar macrophages were isolated from the lungs of SD rats and were confirmed to be macrophages by morphology and CD68 staining

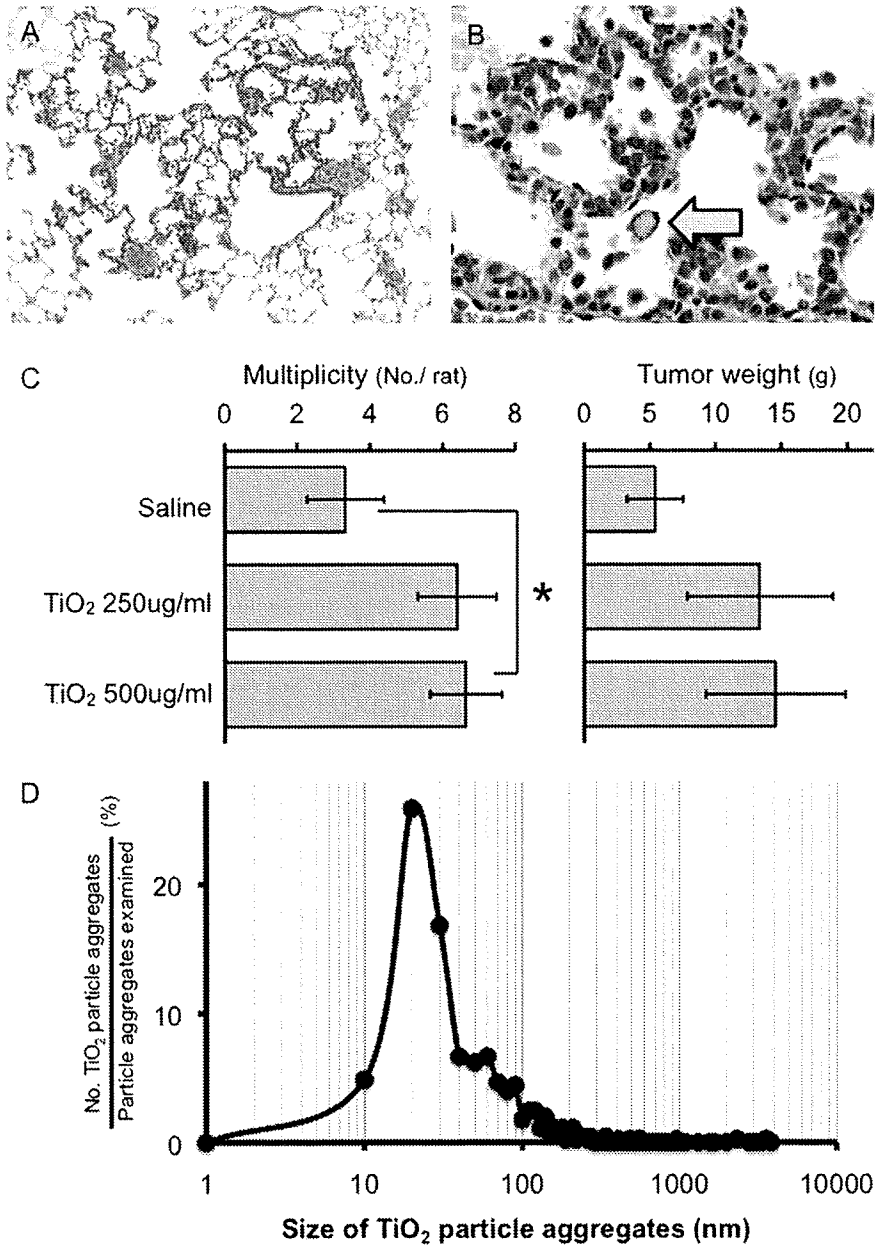


**Fig. 1.** Promoting effects of $TiO_2$ particles in DHPN-induced lung and mammary carcinogenesis (**A**) Alveolar hyperplasias observed in the lung of an H*ras*128 rat receiving DHPN and 500 μg/ml $TiO_2$ particles. (**B**) Alveolar macrophages with $TiO_2$ particles were also observed in hyperplasia lesions. (**C**) IPS of $TiO_2$ particles significantly increased the multiplicity of adenocarcinomas in the mammary gland and tended to increase the size of mammary tumors. (**D**) The size distribution of $TiO_2$ particle aggregates; among 452 particle aggregates examined, 362 (80.1%) were nanosize, i.e. <100 nm in diameter.

(data not shown). The macrophages were treated with $TiO_2$ particles suspended in saline (Figure 4A). $TiO_2$ induced secretion of MIP1α into the culture media (Figure 4B), and the culture medium collected from macrophages treated with $TiO_2$ particles promoted proliferation of A549 cells, whereas culture media collected from unexposed macrophages did not (Figure 4C). MIP1α neutralizing antibodies attenuated the promotion of A549 proliferation in a dose-dependent manner (Figure 4C). MIP1α-induced cell proliferation was also significantly suppressed by the ERK inhibitor PD98059 (Figure 4D). In addition, MIP1α increased ERK phosphorylation and PD98059 diminished ERK phosphorylation (Figure 4E).

We also examined the effect of MIP1α, GRO and IL-6, $H_2O_2$ and $TiO_2$ on the proliferation of A549 cells. MIP1α increased cell proliferation in a dose-dependent fashion, but GRO and IL-6 did not (supplementary Figure 3A–C is available at *Carcinogenesis* Online). $H_2O_2$ significantly suppressed cell proliferation, and antioxidant treatment diminished this suppression. Antioxidant treatment did not affect MIP1α-induced cell proliferation (supplementary Figure 3D is available at *Carcinogenesis* Online). These results suggest that ROS have no effect on tumor cell growth in this experiment.

In addition, $TiO_2$ did not directly increase proliferation of A549 cell (supplementary Figure 3E is available at *Carcinogenesis* Online).

### *Mechanism analysis of the promotion of mammary carcinogenesis*

MIP1α was markedly elevated in the serum of the H*ras*128 rats treated with $TiO_2$ particles (Figure 5A). Serum levels of IL-6 were not changed by $TiO_2$ treatment and GRO was not detected in the serum

**Table I.** Effect of TiO2 on incidence and multiplicity of DHPN-induced alveolar hyperplasia and adenoma of the lung

| Treatment | No. of rats | Alveolar hyperplasia | | Lung adenoma | |
|---|---|---|---|---|---|
| | | Incidence (%) | Multiplicity ## (no./cm$^2$) | Incidence (%) | Multiplicity # (no./cm$^2$) |
| Saline | 9 | 9 (100) | 5.91 ± 1.19 | 0 | 0 |
| n$TiO_2$ 250 mg/ml | 10 | 10 (100) | 7.36 ± 0.97* | 1 (10) | 0.10 ± 0.10 |
| n$TiO_2$ 500 mg/ml | 11 | 11 (100) | 11.05 ± 0.87** | 4 (36) | 0.46 ± 0.21* |

*$P < 0.05$, **$P < 0.001$ versus saline control.
#$P < 0.05$, ##$P < 0.001$ in trend test (Spearman's rank correlation test).

(Figure 5A). MIP1α was slightly elevated in the mammary glands of these animals (Figure 5B); possibly, the elevated MIP1α detected in the mammary tissue was due to contamination by MIP1α in the serum. Recombinant MIP1α promoted the proliferation of C3 cells in a dose-dependent manner; a slight induction could be seen at a dose of 400 pg/ml and became statistically significant at the dose of 50 ng/ml (Figure 5C). Expression of CCR1, the major receptor of MIP1α, was observed in mammary tissue, and as in the lung, IPS of $TiO_2$ particles had little or no effect on CCR1 expression (data not shown). $TiO_2$ did not directly increase proliferation of C3 cells (supplementary Figure 3F is available at *Carcinogenesis* Online).

## Discussion

To elucidate the mechanism underlying rat lung carcinogenesis by $TiO_2$ inhalation, we chose IPS. Although this method may be less physiological than the aerosol inhalation system, we observed that agglomerates and aggregates of $TiO_2$ particles from nano to micro size (mean diameter 107.4 nm) were diffusely distributed throughout the lung including peripheral alveoli, and they did not cause obstruction of the terminal bronchioles. Accordingly, IPS of $TiO_2$ particles can be expected to act similarly to aerosol inhalation of $TiO_2$.

Occupational exposure limits for $TiO_2$ in 13 countries or regions are 5–20 mg/m$^3$ (20), which results in $TiO_2$ exposure limits of 0.27–1.07 mg/kg body wt/day; calculations based on the human respiratory volume. In the present study, a total of 1.75 mg was administered per rat for 12 weeks in the high-dose group, resulting in a dose of 0.104 mg/kg body wt/day. Therefore, the dose we used in the present study was lower than the occupational exposure limit.

$TiO_2$, nanoscale and larger sized is evaluated as a Group 2B carcinogen by World Health Organization/International Agency for Research on Cancer (4) based on 2 year animal aerosol inhalation studies (3). We conducted the present carcinogenesis study using a two-step initiation–promotion protocol as a surrogate for a 2 year long-term protocol. Our study demonstrated that $TiO_2$ particles increased the multiplicity of alveolar cell hyperplasia and adenoma in the two-step IPS-initiation–promotion protocol. We used these lesions as endpoints in carcinogenicity testing because chemically induced tumors appear to be derived from hyperplasic lesions that progress to adenoma and carcinoma (21).

Several bioassay protocols based on the two-step carcinogenesis theory have been developed as practical and sensitive assays, and the compounds that exhibit promotion activity are considered to be carcinogens (22–29). Thus, our experimental design may be a practical surrogate for the long-term lung carcinogenesis protocol.

It should be noted that proliferative lesions including alveolar cell hyperplasia and adenomas were not found in the groups subjected to $TiO_2$ particle administration without prior treatment of DHPN. This is due to the weak carcinogenic potential and short duration of exposure to $TiO_2$ particles. Using the two-step IPS-initiation–promotion protocol, however, we did observe carcinogenic activity by this weak carcinogen. Thus, the two-step IPS-initiation–promotion protocol is an appropriate system to study carcinogenesis of $TiO_2$ particles and approximates long-term $TiO_2$ inhalation studies (3,11).

We next conducted a mechanism analysis of $TiO_2$ particle carcinogenesis focusing on the initial events induced by exposure to $TiO_2$ particles. Treatment with $TiO_2$ resulted in a modest infiltration of inflammatory cells into the alveolar space and septal wall, but the primary effect was a marked increase in the number of macrophages in the alveoli, and many of these macrophages contained phagocytosed $TiO_2$ particles. Alveolar macrophages play an important role in deposition and clearance of mineral fibers/particles, and macrophage activity is known to be strongly associated with inflammatory reactions and carcinogenesis caused by fibers and particles in the lung, including asbestos (30–33). ROS are known to be produced by macrophages upon particle phagocytosis (34,35). Clinical and experimental studies indicate that ROS production and resultant oxidative stress play an important role in cellular and tissue damage, inflammation and fibrosis in the lung. In our study, a significant increase in the activity of SOD and 8-OHdG formation in the lung were observed, indicating increased ROS production and DNA damage. Because macrophages are unable to detoxify $TiO_2$ particles, the reaction against these particles would be continuous over an extended period of time. This condition is associated with high levels of ROS production (36) and tissue toxicity (37).

Cytokine analysis of the lung tissue indicated that among the 12 cytokines examined, expression of IL-6, GRO and MIP1α were significantly higher in the $TiO_2$-treated group than in the vehicle group (supplementary Table 1 is available at *Carcinogenesis* Online). IL-6 is a pro-inflammatory cytokine that is involved in host defense as well as cancer development (38,39). IL-6 has been shown to be increased in lung tumor tissue (40,41) and in the sera of lung cancer patients (42). GRO, a member of the CXC chemokine family, has been shown to be involved in inflammatory responses, chemoattraction (43), carcinogenesis (44,45) and tumor progression (46). Thus, IL-6 and GRO may be involved in the promotion of lung carcinogenesis by $TiO_2$ (47).

Of the three cytokines induced by exposure to $TiO_2$ particles, however, we were particularly interested in MIP1α. This cytokine was not only induced in the lung tissue of $TiO_2$-treated rats, but, unlike IL-6 and GRO, it was also found in the serum of these animals. MIP1α is a member of the CC chemokine family and is primarily associated with cell adhesion and migration (17), proliferation and survival of myeloma cells (48). It is produced by macrophages in response to a variety of mineral particle-induced inflammatory stimuli (18). Our results indicate that expression of MIP1α by alveolar macrophages enhances the proliferation of A549 cells. Expression of CCR1, the major receptor of MIP1α, was observed in the lung tissue, rendering lung cells receptive to MIP1α induction of proliferation. Lung damage and inflammation induced by $TiO_2$ particles has also been reported to be associated with increased cell proliferation of lung epithelium cells (49), which is consistent with our results.

The MEK1–ERK-signaling pathway has been shown to be involved in CCR1 signaling (48). In the present study, the MEK1-specific inhibitor PD98059 suppressed MIP1α-induced cell proliferation and ERK phosphorylation. These results suggest that MEK1 is one of the downstream signaling molecules of MIP1α and the MEK1–ERK-signaling pathway may be partially involved in MIP1α signaling.

It should be noted that, in our IPS-initiation–promotion protocol, $TiO_2$ exposure also promoted DHPN-initiated mammary carcinogenesis. Our results suggest that MIP1α secreted by alveolar macrophages and transported via the circulatory system caused

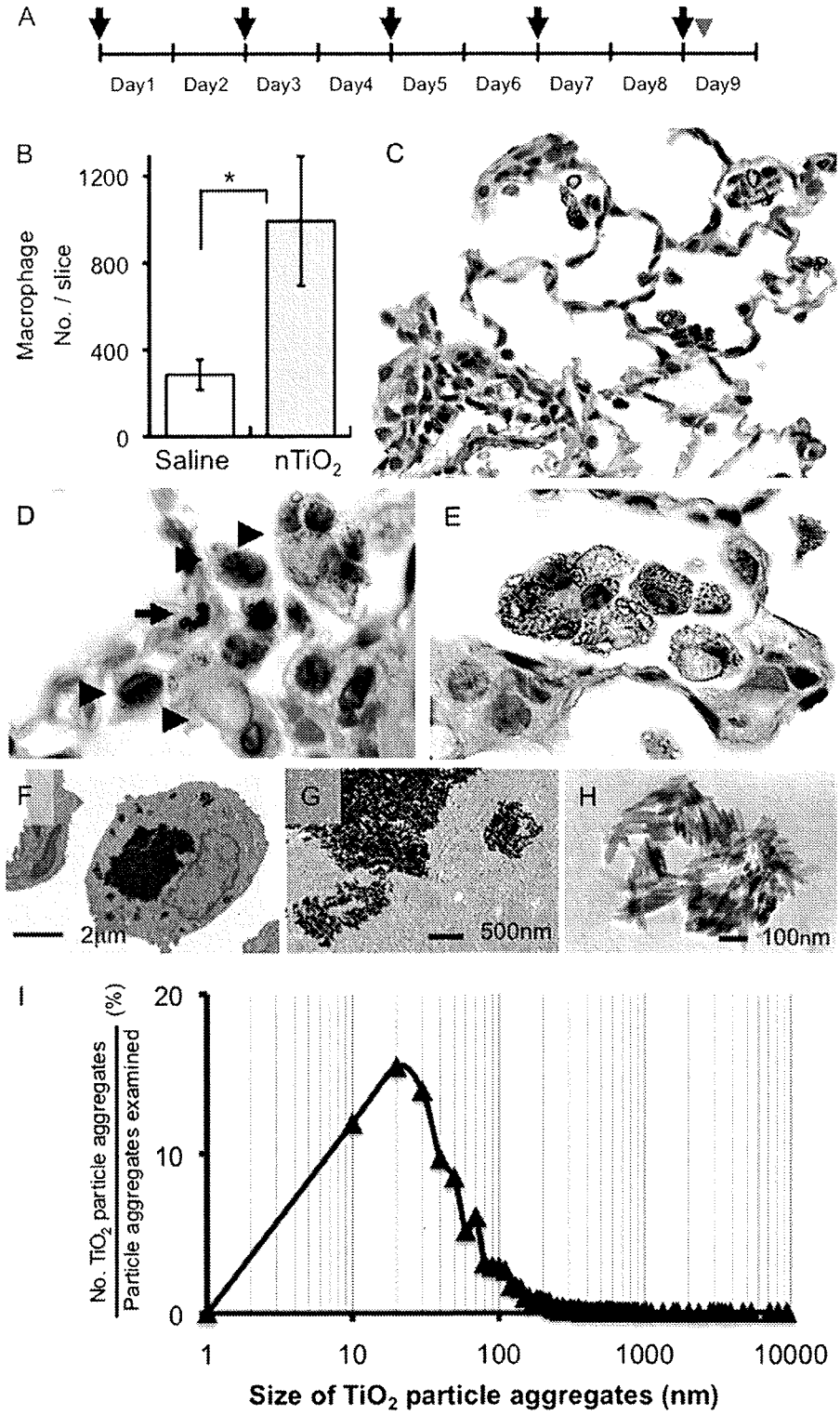


**Fig. 2.** $TiO_2$ particles in alveolar macrophages by light and electron microscopy (**A**) Twenty female SD rats (wild-type counterpart of H*ras*128) aged 10 weeks were treated by IPS with 0.5 ml suspension of 500 μg/ml $TiO_2$ particles in saline five times over a 9 day period. Arrows and arrowhead indicates IPS treatment and killing of the animals, respectively. (**B**) IPS of $TiO_2$ particles significantly increased the number of macrophages in the alveoli. (**C**) Inflammatory reactions were observed in the lung with slight infiltration of macrophages, neutrophils and lymphocytes. (**D**) $TiO_2$ particles were observed in alveolar macrophages (hematoxylin and eosin staining). Arrowheads indicate macrophages and the smaller cell indicated by the arrow is a neutrophil with its characteristic multilobular nucleus. (**E**) The multinucleated cells containing these particles were positive for the macrophage marker CD68 (Alkaline phosphatase reaction, red color). (**F**) TEM findings showed that $TiO_2$ particles of various sizes (~50 nm to 5 μm) were observed phagocytosed by alveolar macrophages. (**G**) Electron dense bodies were aggregates of $TiO_2$ particles. (**H**) TEM findings of $TiO_2$ particles in saline suspension before IPS. The shape of the $TiO_2$ particle aggregates was similar to those observed in macrophages. (**I**) The size distribution of $TiO_2$ particle aggregates: of 2571 particle aggregates examined, 1970 (77.1%) were <100 nm. The average size was 107.4 nm and the median size was 48.1 nm.

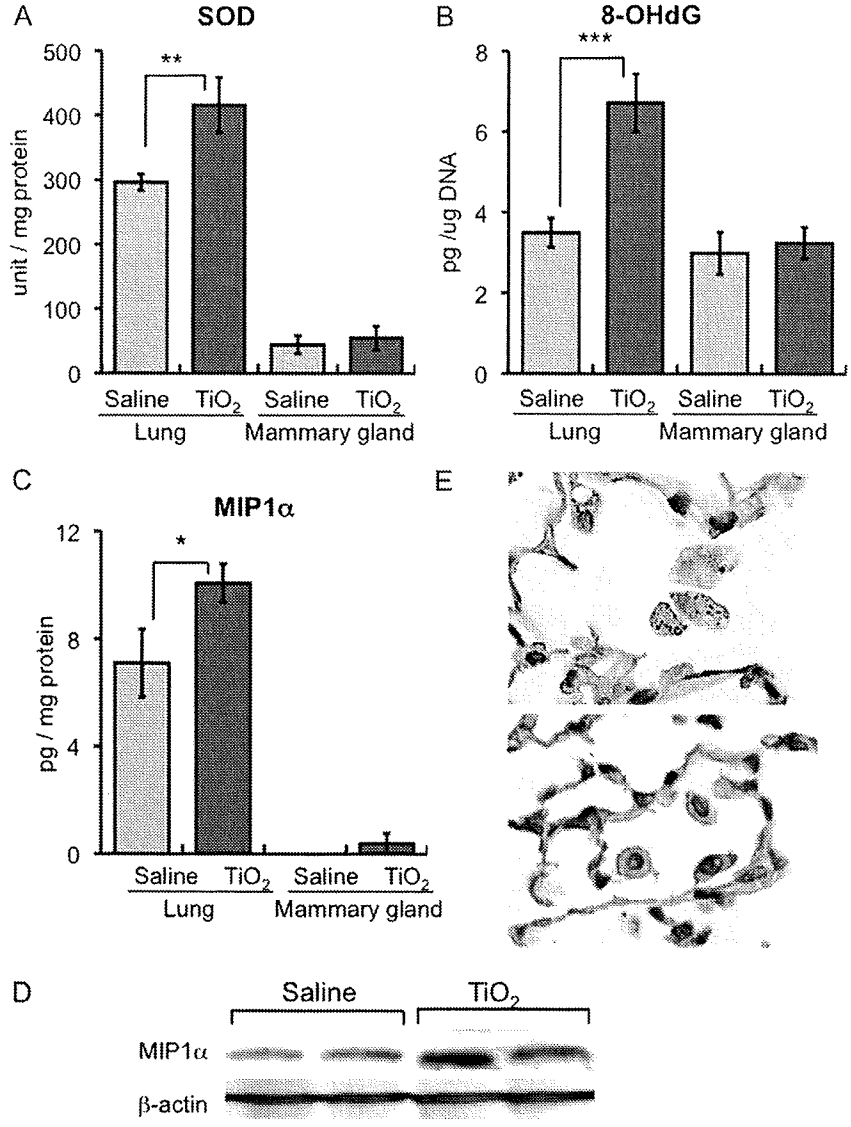


**Fig. 3.** Inflammatory factors upregulated in the lungs of wild-type rats by IT-spraying of $TiO_2$ particles in the IPS 9 day study (**A**) SOD activity and (**B**) 8-OHdG level in wild-type rats treated with $TiO_2$ particles or saline. (**C**) MIP1α protein level was significantly increased (142%) in the lung tissue of wild-type rats treated with $TiO_2$ (suspension array analysis). MIP1α was detected in the mammary gland of the $TiO_2$ group but not in the vehicle group. (**D**) In western blotting, expression of MIP1α was increased in the $TiO_2$ group compared with vehicle group. (**E**) MIP1α was immunohistochemically detected in alveolar macrophages containing $TiO_2$ particles (upper) but was not detected in macrophages of rats that were not exposed to $TiO_2$ particles (lower).

proliferation of mammary epithelial cells and thereby promoted mammary carcinogenesis. As with the lung, CCR1 was expressed by mammary cells, rendering these cells receptive to MIP1α induction of proliferation. While MIP1α secreted by alveolar macrophages would be diluted by the blood volume and while these levels may not be high enough to increase mammary cell proliferation in a short *in vitro* proliferation assay, it is possible that continuous low level stimulation over the course of 12 weeks could increase mammary cell proliferation in the environment of the mammary gland *in vivo*. Another possibility is that $TiO_2$ particles may act directly on the mammary gland after translocation to the mammary gland from the lung. However, $TiO_2$ exposure of mammary carcinoma cells did not induce proliferation *in vitro*. It must be understood that promotion of DHPN-induced mammary carcinogenesis by $TiO_2$ particles was observed in H*ras*128 female rats, and these animals are very highly susceptible to mammary carcinogenesis (50). Although, the effects we observed on promotion of mammary carcinogenesis in these animals may not be directly relevant to most humans, people at high risk for mammary carcinogenesis, such as individuals harboring BRCA mutations, may be a relevant population as regards the risk presented by nanoscale $TiO_2$.

Although our observations are based on results obtained with a mixed population of nanoscale and larger sized particle aggregates, size analysis indicated that 80.1% of them were nanoscale (<100 nm in diameter) in the 16 week IPS-initiation–promotion study and 76.6% were nanoscale in the IPS 9 day study. Thus, the results can be interpreted as being strongly associated with nanoscale particle aggregates.

In conclusion, the IPS-initiation–promotion protocol detected $TiO_2$ carcinogenic activity in the rat lung and is therefore comparable, at least for $TiO_2$ inhalation, to a long-term whole body inhalation carcinogenesis study. We also elucidated a plausible mechanism for the carcinogenic effect of $TiO_2$ particles in the rat lung. Phagocytosis of $TiO_2$ particles by alveolar macrophages resulted in ROS production and DNA damage and increased expression of MIP1α. MIP1α in turn was able to enhance proliferation of lung epithelium cells. Thus, lung

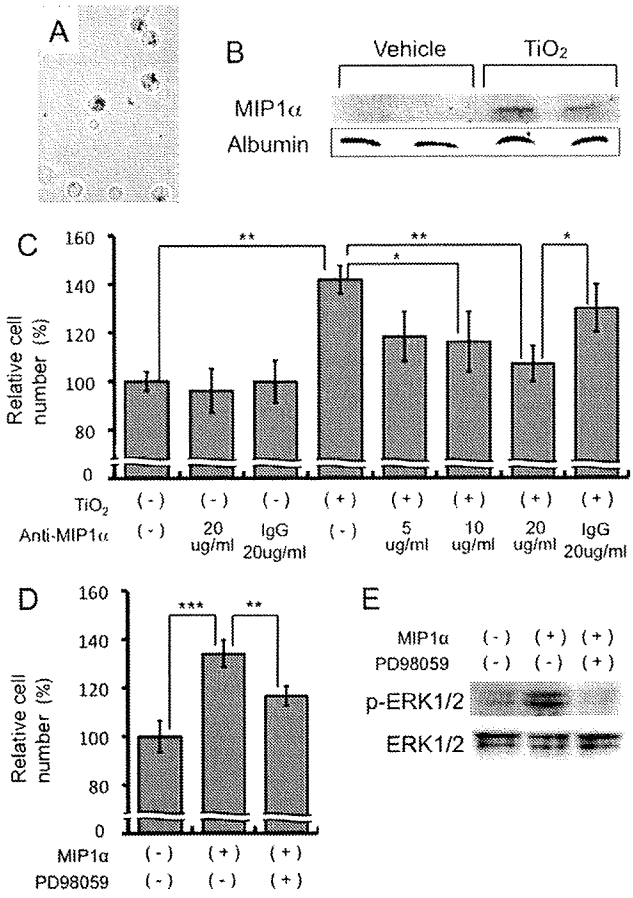


**Fig. 4.** Growth stimulation effects of conditioned medium from alveolar macrophages on human lung cancer cell lines. (**A**) Primary cultured alveolar macrophages of rats were treated with $TiO_2$ particles. (**B**) MIP1α was detected in the culture medium. (**C**) The number of A549 cells was significantly increased by addition of conditioned medium from alveolar macrophages treated with $TiO_2$ particles. MIP1α neutralizing antibody attenuated this effect in a dose-dependent manner. Irrelevant IgG was used as control antibody. (**D**) MIP1α-induced cell proliferation was significantly suppressed by the ERK inhibitor PD98059. (**E**) MIP1α increased ERK phosphorylation and PD98059 diminished this phosphorylation.

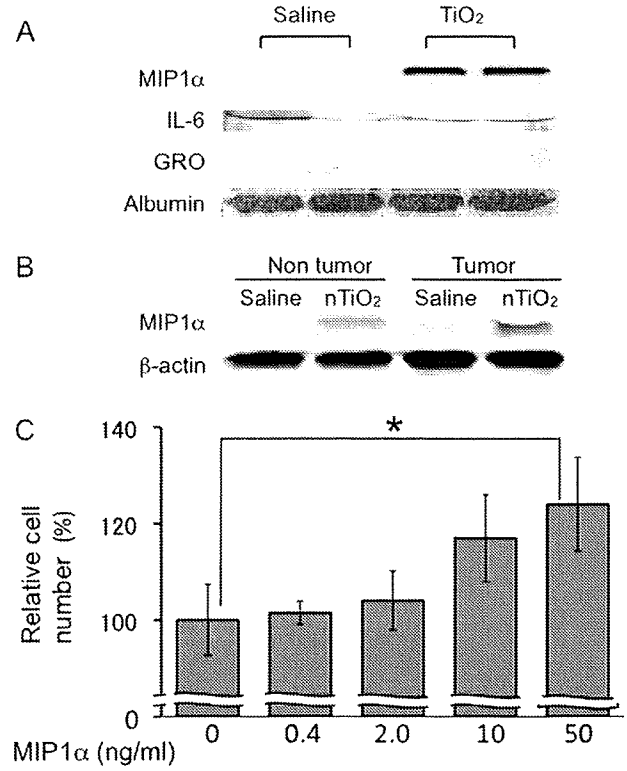


**Fig. 5.** Promotion effects of MIP1α on proliferation of a rat mammary cancer cell line, C3 (**A**) MIP1α was detected in the serum of the H*ras*128 rats treated with $TiO_2$ but not in vehicle control rats in the 16 week study. No difference in IL-6 in the serum was observed and GRO was not detected in the serum. (**B**) MIP1α levels are slightly elevated in non-tumor and tumor tissue of the mammary gland of animals treated by IPS with $TiO_2$ particles in the 16 week study. (**C**) Recombinant MIP1α increased the number of rat mammary carcinoma C3 cells in a dose-dependent manner ($P$ = 0.0127).

tissue exposed to $TiO_2$ particles exhibits increase in both DNA damage and proliferation. Importantly, a similar mechanism would function in humans in the promotion of lung carcinogenesis associated with inhalation of $TiO_2$ particles and other nanoparticles with the capacity to form aggregates. In addition, $TiO_2$ administered to the lung had carcinogenic activity in the H*ras*128 transgenic rat mammary gland; this carcinogenic activity is probably mediated via serum MIP1α resulting from expression of MIP1α by alveolar macrophages. This finding may indicate that exposure of $TiO_2$ particles is a risk factor for mammary carcinogenesis in predisposed populations, such as individuals with BRCA mutations.

## Supplementary material

Supplementary Figures 1–3 and Tables 1 and 2 can be found at http://carcin.oxfordjournals.org/

## Funding

Health and Labour Sciences Research Grants, Ministry of Health, Labour and Welfare, Japan (Research on Risk of Chemical Substance 21340601, H18-kagaku-ippan-007); a grant-in-aid for the Second Term Comprehensive 10 Year Strategy for Cancer Control, Ministry of Health, Labour and Welfare, Japan; grants-aid for Cancer Research, Ministry of Education, Culture, Sports, Science and Technology.

## Acknowledgements

*Conflict of Interest Statement:* None declared.

## References

1. Oberdorster,G. (2002) Toxicokinetics and effects of fibrous and nonfibrous particles. *Inhal. Toxicol.*, **14**, 29–56.
2. Romundstad,P. *et al.* (2001) Cancer incidence among workers in the Norwegian silicon carbide industry. *Am. J. Epidemiol.*, **153**, 978–986.
3. Pott,F. *et al.* (2005) Carcinogenicity study with nineteen granular dusts in rats. *Eur. J. Oncol.*, **10**, 249–281.
4. Baan,R. *et al.* (2006) Carcinogenicity of carbon black, titanium dioxide, and talc. *Lancet Oncol.*, **7**, 295–296.
5. Schulte,P. *et al.* (2008) Occupational risk management of engineered nanoparticles. *J. Occup. Environ. Hyg.*, **5**, 239–249.
6. Maynard,A.D. *et al.* (2006) Safe handling of nanotechnology. *Nature*, **444**, 267–269.
7. Scheringer,M. (2008) Nanoecotoxicology: environmental risks of nanomaterials. *Nat. Nanotechnol.*, **3**, 322–323.
8. Borm,P. *et al.* (2006) Research strategies for safety evaluation of nanomaterials, part V: role of dissolution in biological fate and effects of nanoscale particles. *Toxicol. Sci.*, **90**, 23–32.
9. Phalen,R.F. (1976) Inhalation exposure of animals. *Environ. Health Perspect.*, **16**, 17–24.

10. Mauderly,J.L. (1997) Relevance of particle-induced rat lung tumors for assessing lung carcinogenic hazard and human lung cancer risk. *Environ. Health Perspect.*, **105** (suppl. 5), 1337–1346.
11. Roller,M. *et al.* (2006) Lung tumor risk estimates from rat studies with not specifically toxic granular dusts. *Ann. N. Y. Acad. Sci.*, **1076**, 266–280.
12. Imaida,K. *et al.* (1996) Initiation-promotion model for assessment of carcinogenicity: medium-term liver bioassay in rats for rapid detection of carcinogenic agents. *J. Toxicol. Sci.*, **21**, 483–487.
13. IARC (1999) The use of short-and medium-term tests for carcinogens and data on genetic effects in carcinogenic hazard evaluation. Consensus report. *IARC Sci. Publ.*, **146**, 1–18.
14. Asamoto,M. *et al.* (2000) Transgenic rats carrying human c-Ha-ras proto-oncogenes are highly susceptible to N-methyl-N-nitrosourea mammary carcinogenesis. *Carcinogenesis*, **21**, 243–249.
15. Han,B.S. *et al.* (2002) Inhibitory effects of 17beta-estradiol and 4-n-octylphenol on 7,12-dimethylbenz[a]anthracene-induced mammary tumor development in human c-Ha-ras proto-oncogene transgenic rats. *Carcinogenesis*, **23**, 1209–1215.
16. Ohnishi,T. *et al.* (2007) Possible application of human c-Ha-ras proto-oncogene transgenic rats in a medium-term bioassay model for carcinogens. *Toxicol. Pathol.*, **35**, 436–443.
17. Terpos,E. *et al.* (2005) Significance of macrophage inflammatory protein-1 alpha (MIP-1alpha) in multiple myeloma. *Leuk. Lymphoma*, **46**, 1699–1707.
18. Driscoll,K.E. *et al.* (1993) Macrophage inflammatory proteins 1 and 2: expression by rat alveolar macrophages, fibroblasts, and epithelial cells and in rat lung after mineral dust exposure. *Am. J. Respir. Cell Mol. Biol.*, **8**, 311–318.
19. Hamaguchi,T. *et al.* (2006) Establishment of an apoptosis-sensitive rat mammary carcinoma cell line with a mutation in the DNA-binding region of p53. *Cancer Lett.*, **232**, 279–288.
20. IARC (1989) Titanium dioxide. *IARC monograph Evaluation of carcinogenic risks to humans*. IARC Scientific Publications, Lyon, vol. 47, pp. 307–326.
21. Stoner,G.D. *et al.* (1993) Lung tumors in strain A mice: application for studies in cancer chemoprevention. *J. Cell. Biochem. Suppl.*, **17F**, 95–103.
22. Pitot,H.C. *et al.* (1978) Biochemical characterisation of stages of hepatocarcinogenesis after a single dose of diethylnitrosamine. *Nature*, **271**, 456–458.
23. Peraino,C. *et al.* (1971) Reduction and enhancement by phenobarbital of hepatocarcinogenesis induced in the rat by 2-acetylaminofluorene. *Cancer Res.*, **31**, 1506–1512.
24. Ito,N. *et al.* (2003) A medium-term rat liver bioassay for rapid *in vivo* detection of carcinogenic potential of chemicals. *Cancer Sci.*, **94**, 3–8.
25. Ito,N. *et al.* (1988) Wide-spectrum initiation models: possible applications to medium-term multiple organ bioassays for carcinogenesis modifiers. *Jpn. J. Cancer Res.*, **79**, 413–417.
26. IARC (1980) Long-term and short-term screening assays for carcinogens: a critical appraisal. *IARC Scientific Publications, Lyon, vol.* 83 (suppl. 2), pp. 1–146.
27. Konishi,Y. *et al.* (1987) Lung carcinogenesis by N-nitrosobis(2-hydroxypropyl)amine-related compounds and their formation in rats. *IARC Sci. Publ.*, **82**, 250–252.
28. Nishikawa,A. *et al.* (1994) Effects of cigarette smoke on N-nitrosobis(2-oxopropyl)amine-induced pancreatic and respiratory tumorigenesis in hamsters. *Jpn. J. Cancer Res.*, **85**, 1000–1004.
29. Yamanaka,K. *et al.* (1996) Exposure to dimethylarsinic acid, a main metabolite of inorganic arsenics, strongly promotes tumorigenesis initiated by 4-nitroquinoline 1-oxide in the lungs of mice. *Carcinogenesis*, **17**, 767–770.
30. Rom,W.N. *et al.* (1991) Cellular and molecular basis of the asbestos-related diseases. *Am. Rev. Respir. Dis.*, **143**, 408–422.
31. Heppleston,A.G. (1984) Pulmonary toxicology of silica, coal and asbestos. *Environ. Health Perspect.*, **55**, 111–127.
32. Renwick,L.C. *et al.* (2001) Impairment of alveolar macrophage phagocytosis by ultrafine particles. *Toxicol. Appl. Pharmacol.*, **172**, 119–127.
33. Rimal,B. *et al.* (2005) Basic pathogenetic mechanisms in silicosis: current understanding. *Curr. Opin. Pulm. Med.*, **11**, 169–173.
34. Wang,Y. *et al.* (2007) The role of the NADPH oxidase complex, p38 MAPK, and Akt in regulating human monocyte/macrophage survival. *Am. J. Respir. Cell Mol. Biol.*, **36**, 68–77.
35. Bhatt,N.Y. *et al.* (2002) Macrophage-colony-stimulating factor-induced activation of extracellular-regulated kinase involves phosphatidylinositol 3-kinase and reactive oxygen species in human monocytes. *J. Immunol.*, **169**, 6427–6434.
36. Dorger,M. *et al.* (2000) Comparison of the phagocytic response of rat and hamster alveolar macrophages to man-made vitreous fibers *in vitro*. *Hum. Exp. Toxicol.*, **19**, 635–640.
37. Blake,T. *et al.* (1998) Effect of fiber length on glass microfiber cytotoxicity. *J. Toxicol. Environ. Health A*, **54**, 243–259.
38. Kabir,S. *et al.* (1995) Serum levels of interleukin-1, interleukin-6 and tumour necrosis factor-alpha in patients with gastric carcinoma. *Cancer Lett.*, **95**, 207–212.
39. Schneider,M.R. *et al.* (2000) Interleukin-6 stimulates clonogenic growth of primary and metastatic human colon carcinoma cells. *Cancer Lett.*, **151**, 31–38.
40. Asselin-Paturel,C. *et al.* (1998) Quantitative analysis of Th1, Th2 and TGF-beta1 cytokine expression in tumor, TIL and PBL of non-small cell lung cancer patients. *Int. J. Cancer*, **77**, 7–12.
41. Matanic,D. *et al.* (2003) Cytokines in patients with lung cancer. *Scand. J. Immunol.*, **57**, 173–178.
42. Brichory,F.M. *et al.* (2001) An immune response manifested by the common occurrence of annexins I and II autoantibodies and high circulating levels of IL-6 in lung cancer. *Proc. Natl Acad. Sci. USA*, **98**, 9824–9829.
43. Rollins,B.J. (1997) Chemokines. *Blood*, **90**, 909–928.
44. Zhou,Y. *et al.* (2005) The chemokine GRO-alpha (CXCL1) confers increased tumorigenicity to glioma cells. *Carcinogenesis*, **26**, 2058–2068.
45. Yang,G. *et al.* (2006) The chemokine growth-regulated oncogene 1 (Gro-1) links RAS signaling to the senescence of stromal fibroblasts and ovarian tumorigenesis. *Proc. Natl Acad. Sci. USA*, **103**, 16472–16477.
46. Li,A. *et al.* (2004) Constitutive expression of growth regulated oncogene (gro) in human colon carcinoma cells with different metastatic potential and its role in regulating their metastatic phenotype. *Clin. Exp. Metastasis*, **21**, 571–579.
47. Rollins,B.J. (2006) Inflammatory chemokines in cancer growth and progression. *Eur. J. Cancer*, **42**, 760–767.
48. Lentzsch,S. *et al.* (2003) Macrophage inflammatory protein 1-alpha (MIP-1 alpha) triggers migration and signaling cascades mediating survival and proliferation in multiple myeloma (MM) cells. *Blood*, **101**, 3568–3573.
49. Baggs,R.B. *et al.* (1997) Regression of pulmonary lesions produced by inhaled titanium dioxide in rats. *Vet. Pathol.*, **34**, 592–597.
50. Tsuda,H. *et al.* (2001) High susceptibility of transgenic rats carrying the human c-Ha-ras proto-oncogene to chemically-induced mammary carcinogenesis. *Mutat. Res.*, **477**, 173–182.

*Received September 27, 2009; revised January 14, 2010; accepted January 24, 2010*

MINI-REVIEW

# Toxicology of Engineered Nanomaterials - A review of Carcinogenic Potential

**Hiroyuki Tsuda[1,2]*, Jiegou Xu[2], Yuta Sakai[3], Mitsuru Futakuchi[2], Katsumi Fukamachi[2]**

## Abstract

**Nanotechnology has considerable socioeconomic potential. Benefits afforded by engineered nanoparticles (NP: defined as being less than 100 nm in diameter) are expected to be significant in fields such as plastics, energy, electronics, aerospace and medicine. However, NPs are being introduced into the market without adequate assessment of their potential toxicities. It is urgently important to conduct risk assessment of commercial NPs and establish a framework enabling risk management which is not subordinate to their commercial production. An overview of currently available carcinogenicity risk evaluation results of NP materials raises serious questions as to their safety. NP sized titanium dioxide ($nTiO_2$) and carbon black (nCB) are carcinogenic to the lung of female rats, and the tumors preferentially include squamous cell morphology. Carbon nanotubes (CNT) induce mesotheliomas when applied intraperitoneally in rats and mice. Data for Fullerenes are insufficient to evaluate carcinogenic risk. Sub-chronic toxicity data indicate that, in general, NPs form aggregates and agglomerates and cause foreign body reactions at their applied sites with inflammatory cell, including macrophage, infiltration. These findings are similar to the biological effects of asbestos, a potent carcinogen, and indicate that careful assessment of NPs is indispensable.**

**Key words:** Nanoparticles - toxicology - carcinogenicity - titanium dioxide - carbon black

*Asian Pacific J Cancer Prev,* **10**, 975-980

## Principles of Safety

The safety of our living environment can be secured by the balanced function of three elements: risk assessment, risk management and risk communication (Figure 1). The first of these elements, risk assessment, must be addressed first, since without reliable risk assessment, risk communication and risk management can not function. Importantly, for reliable risk assessment long-term animal studies are indispensable.

These principles, of course, hold true for engineered nanoparticles. Unfortunately, the risk assessment data for engineered nanoparticles are rather fragmentary. However, the available findings do present a disturbing picture of potential carcinogens entering the market place. Engineered nanoparticles included in this review include nano-size titanium dioxide (nTiO2), carbon black (nCB), single-walled carbon nanotubes (SWCNT), multiple-walled carbon nanotubes (MWCNT) and fullerenes (C60).


**Figure 1. Principles of Safety of the Living Environment.** Safety of the living environment can be secured by the balanced function of three elements: risk assessment, risk management and risk communication

## Metals and Metal-derived Nanoparticles: Titanium dioxide ($nTiO_2$)

In an inhalation study, female rats were exposed to air containing $nTiO_2$ (28nm in diameter) at a concentration of 7.5 mg/m3 for 4 months, then at a concentration of 15 mg/m3 for 4 months, and finally at a concentration of 10 mg/m3 for 16 months, then killed at month 30. The incidence of lung tumors (19%), benign and malignant squamous and alveolar cell tumors combined, were significantly increased compared to the clean air control group (0.5%) (Heinrich et al., 1995).

*[1]Nanotoxicology Project, [2]Department of Molecular Toxicology, Nagoya City University Graduate School of Medical Sciences, [3]Department of Drug Metabolism and Disposition, Nagoya City University Graduate School of Pharmacological Sciences, Nagoya, Japan *For correspondence: a*

In another study, female rats were administered $nTiO_2$ by intratracheal instillation. In this study, several dosing strategies were used. Hydrophilic nano-sized nTiO2 (21-25 nm in diameter) was applied in 5 doses of 3 mg each, 5 doses of 6 mg each, or 10 doses of 6 mg each. Hydrophobic nano-sized $nTiO_2$ (21 nm in diameter) was applied in 15 doses of 0.5 mg each or 30 doses of 0.5 mg each. Hydrophilic anatase $nTiO_2$ (200 nm in diameter) was applied in 10 doses of 6 mg each or 20 doses of 6 mg each. The $nTiO_2$, hydrophilic and hydrophobic $nTiO_2$ and hydrophilic anatase $nTiO_2$, was suspended in PBS with 0.5% Tween 80. The instillation was done once weekly. The animals were observed for up to 30 weeks. The incidences of lung tumors (52-69.6%), adenomas/carcinomas and squamous cell epitheliomas/carcinomas combined, in rats receiving hydrophilic $nTiO_2$ were significantly increased over untreated controls (0%). Anatase $nTiO_2$ also induced significant incidences of lung tumors (29.5-63.6%), and these tumors were similar to those induced by hydrophilic $nTiO_2$. The incidences of benign and malignant lung tumors in the hydrophobic $nTiO_2$ groups (6.7%) was not significant (Pott and Roller, 2005).

In another inhalation study, female rats were treated with $TiO_2$ (size, not indicated) at a concentration of 11.3mg/m3 for 24 months followed by observation for 6 months. Incidences of cystic keratinizing epitheliomas (11.7%) and squamous cell carcinomas (4.8%) were significantly greater than the control group (0.5%) (Rittinghausen et al., 1997). $nTiO_2$ is not carcinogenic to the skin because it does not penetrate the dermal tissue (Newman et al., 2009). Based on the studies outlined here, $nTiO_2$ is evaluated by WHO/IARC as a Group 2B compound (possibly carcinogenic to humans) (Baan, 2007).

## Carbon-derived Nanoparticles

*1. Carbon black (nCB)*

Because of its long history of production and consumption, the highest number of reports concerning the carcinogenicity of carbon-derived nanomaterials are about nCB.

a) Rat studies. In an inhalation study, female rats were exposed to nCB (Printex90, 14 nm in diameter) at a concentration of 7.5 mg/m3 for 4 months and then at a concentration of 12 mg/m3 for 20 months followed by clean air for 6 months. The incidence of lung tumors (39%), benign and malignant squamous cell tumors and bronchio-alveolar cell tumors combined, was significantly increased as compared to the clean air group (0.5%) (Heinrich et al., 1995).

In another study, nCB (Printex90, 14 nm in diameter and Lamp Black101, 98nm in diameter) was administered to female Wistar rats by intratracheal instillation. Printex90 was washed in boiling toluene and suspended in saline containing 0.25% Tween 80. The Printex90 was administered once per week for 3 weeks at a dose of 0.66 mg per rat for 3 weeks then once per week for 13 weeks at a dose of 1.0 mg per rat. Animals were observed for up to 800 days from the beginning of the study. The incidence of cystic keratinizing epitheliomas and bronchio-alveolar cell tumors combined in Printex90 treated rats (21%) was similar to that observed in rats treated with benzo[a]pyrene and diesel emission particles and significantly elevated compared to the vehicle control group (0%). Lamp Black 101 treated rats also showed a significant increase in lung tumors compared to the control group (Dasenbrock et al., 1996).

In a second inhalation study, female Wistar rats were exposed to nCB (Printex90, 14 nm in diameter) at a concentration of 11.3 mg/m3 for four months and then at a concentration of 12.2 mg/m3 for the following 20 months. The incidence of cystic keratinizing tumors (20%), epitheliomas and carcinomas combined, was significantly increased compared to the clean air control group (0%) (Rittinghausen et al., 1997).

In the same series of experiments as the one outlined above, Printex90 was administered to female Wistar rats by intratracheal instillation. Printex90 was suspended in saline with 0.25% Tween 80 and administered 16-17 times (total dose 15 mg per animal). Animals were observed for up to 24 months. In rats receiving Printex90, the incidence of cystic keratinizing epitheliomas (19%) was significantly increased compared to saline treated animals (0%). Rats were also treated with purified Lamp Black: the treatment regimen was the same as for Printex90. Tumor incidence in these rats (6.3%) was not significantly elevated (Rittinghausen et al., 1997).

In a fifth study, nCB (Printex90, 14 nm in diameter and Lamp Black 101, 98nm in diameter; Degussa) was administered to female Wistar rats by intratracheal instillation. Printex90 was washed in boiling toluene and suspended in saline containing 0.25% Tween 80. The Printex90 was applied once per week for 3 weeks at a dose of 0.66 mg per rat for 3 weeks then once per week for 13 weeks at a dose of 1.0 mg per rat. Animals were observed for up to 800 days from the beginning of the study. The incidence of cystic keratinizing epitheliomas and bronchio-alveolar cell tumors combined in Printex90 treated rats (21%) was similar to that observed in rats treated with benzo[a]pyrene and diesel emission particles and significantly elevated compared to the vehicle control group (0%). Lamp Black101 treated rats also showed a significant increase in lung tumors compared to the control group (Dasenbrock et al., 1996).

In a sixth study, nCB (Printex90 or purified Lamp Black 101) was administered to female SPF Wistar rats intratracheal instillation. Animals were observed for up to 30 months. Several dosing strategies were used: animals were treated from 5 to 20 times with 1.5 to 6 mg nCB. Total lung tumor incidence for each treatment regimen (Printex90, 56% to over 80%; Lamp Black, 44% to 70%) was significantly elevated compared to the control group (2%) (Pott and Roller, 2005).

Based on the studies outlined here, nCB is evaluated by WHO/IARC as a Group 2B compound (possibly carcinogenic to humans) (Baan, 2007).

b) Mouse and Hamster Studies. No data are available as to carcinogenicity and related studies in mice and hamsters.

c) Summary. nCB is carcinogenic to the female rat inducing cystic keratinizing epitheliomas and bronchio-alveolar cell lung tumors. Mechanisms to explain why cystic squamous cell tumors were induced exclusively in female rats have not yet been elucidated. No data for carcinogenicity of nCB in mice and hamsters are available.

*2. Carbon nanotubes*

There are two types of carbon nanotubes: single-walled carbon nanotubes (SWCNT) are tube structures with a diameter of close to 1 nanometer and composed of a one-atom-thick layer of graphite (Figure 2, left), and multi-walled carbon nanotubes (MWCNT) are tube structures with a diameter of close to 1 nanometer and composed of two or more layers of graphite atoms (Figure 2, right).

A) SWCNT; a) Rat studies. In a short to medium-term (6 months or less) study, SWCNT (diameter 1.4 nm, length more than 1 mm agglomerate at use) was administered to male Crl:CD(SD)IGS BR rats intratracheal instillation. The SWCNT particles were suspended in PBS with 1% Tween 80 and administered one time at 1 or 5 mg/kg. Animals were observed up to 12 weeks. Multifocal small granulation tissue with deposition of aggregates of SWCNT were observed in the lung. Inflammatory cell counts of bronchoalveolar lavage (BAL) did not clearly correlate with the degree of the inflammatory reaction. Similar inflammatory changes were also observed in rats which received quarts particles (crystalline, diameter 1-3 mm). No tumors were found in any of the groups (Warheit et al., 2004).

b) Mouse studies. In a short to medium-term (6 months or less) study, SWCNT (diameter 0.8-2.2 nm, length not indicated) and cup-stacked CNT (mean diameter 80 nm, length not more than 100 mm) were administered to female BALB/c mice by subcutaneous injection. The SWCNT and CNT particles were suspended in saline and animals were injected at 2 mg per animal then observed for up to 12 weeks. The iron content of these materials was 3.5-5.0% (weight). Although inflammatory lesions in the injected site were observed, no tumors were found (Koyama et al., 2006).

In another short to medium-term (6 months or less) study, SWCNT (iron content, 26.9% weight) was administered to male B6C3F1 mice by intratracheal instillation. Unpurified SWCNT and purified (polycyclic aromatic hydrocarbon-free) SWCNT suspended in heat-inactivated mouse serum at a concentration of 2 mg/ml was administered one time at 0.1 or 0.5 ml/mouse. The animals were then observed for 7 or 90 days. Granulation tissue formation with epithelioid cell reaction was observed in the bronchioles, respiratory ducts and alveoli. The inflammatory reaction in animals given SWCNT was more prominent than animals treated with carbon black. Neoplastic lesion development was not observed (Lam et al., 2004).

B) MWCNT: a) Rat studies. In a short to medium-term (6 months or less) study, MWCNT (average 15 carbon layers, approximate inner diameter 5 nm, outer diameter 9-10 nm) was administered to female SD rats by intratracheal instillation. The MWCNT particles were suspended in saline with 1% Tween 80 and administered one time at doses of 0.5, 2.0 and 5 mg/rat in 0.5 ml saline. The rats were killed on day 60. Small granulation tissue with deposition of MWCNT was observed in the bronchi, bronchio-alveolar space and some alveoli. No tumors were found (Muller et al., 2005).

In another study, MWCNT (MUTSUI MWCNT-7, 3500 ppm iron content; diameter 70-100 nm; approximate length 1-4 micrometers) was administered to male F344/DuCrlj rats by a single intrascrotal injection. The MWCNT particles were suspended in 0.5% methyl cellulose with 1.0% Tween 80 and administered at a dose of 20 mg/mouse. The animals were then observed until week 104. Another group of mice were treated with crocidolite (UICC grade asbestos). The incidence of disseminated mesothelioma in the peritoneal cavity was 86% in MWCNT and 0% in crocidolite groups (Sakamoto et al., 2009).

In a third study, MWCNT (11.3 nm in mean diameter, approximate length 0.7 micrometers) was administered to three groups of male Wistar rats by a single intraperitoneal injection. MWCNT with structural defects was suspended in PBS and administered at a dose of 2 or 20 mg/rat and MWCNT without structural defects was suspended in PBS and administered at a dose of 20 mg/rat. The animals were then observed for up to 104 weeks. Another group of rats was treated with 2 mg crocidolite (UICC grade asbestos) per rat. The incidence of mesothelioma in the group administered crocidolite was 34.6%, but the incidence of mesothelioma in the MWCNT groups (up to 6%) was not statistically higher than the incidence (3.8%) in the vehicle control group (Muller et al., 2009).

b) Mouse studies. In a short to medium-term (6 months or less) study, MWNT (diameter 20-150 nm, length 10-20 mm) was administered to female BALB/c mice by a single subcutaneous injection. The nano-particles were suspended in saline administered at 2 mg per mouse. The animals were then observed for up to 12 weeks. The iron content of these materials was 3.5-5.0% (weight). Although

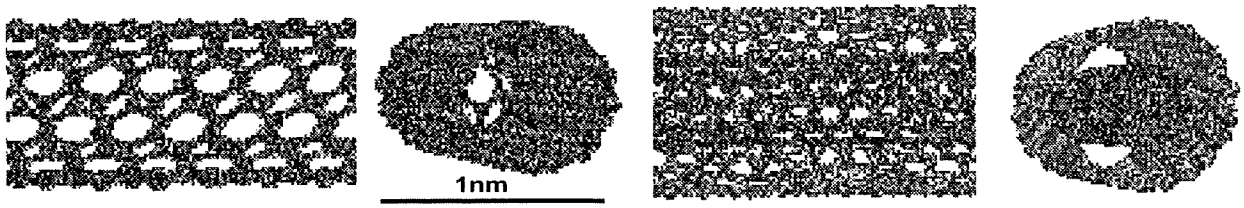


**Figure 2. Structure of a Single-walled Carbon Nanotube (SWCNT) and a Multiple-walled Carbon Nanotube (MWCNT).** (Courtesy of Dr. M. Ata; National Institute of Advanced Industrial Science and Technology, Japan)

inflammatory lesions at the injected site were observed, no tumors were found (Koyama et al., 2006).

In another short to medium-term (6 months or less) study, two types of MWCNT, pure MWCNT and N-doped (nitrogen attached on the surface) MWCNT (approximately 30-50 nm in diameter and 100-300 mm in length) were administered intranasally, intratracheally, orally or intraperitoneally to male CD1 mice. The MWCNT particles were suspended in phosphate buffered saline (PBS) and administered one time at doses of 1, 2.5 or 5 mg/mouse. The animals were killed after 30 days. Intratracheal administration of MWCNT resulted in inflammatory lesions surrounding aggregates of MWCNT and hyperplastic change of the bronchial epithelium in a dose dependent manner. These changes were less intense in N-doped MWCNT. No obvious clinical symptoms were noted in mice treated though other routes (Carrero-Sanchez et al., 2006).

In a third study, MWCNT (MUTSUI MWCNT-7, 3500 ppm iron content; diameter 100 nm; approximate length 1-5 micrometers) was administered to male p53 (+/-) mouse with a C57BL/6background by intraperitoneal injection. The MWCNT was suspended in 0.5% methyl cellulose with 1.0% Tween 80 and administered one time at a dose of 3 mg/mouse. The animals were then observed for 25 weeks. Other groups of mice were treated with C60 and crocidolite (UICC grade asbestos) at a dose of 3 mg/mouse. The incidence of mesothelioma in the peritoneal cavity was 14/16 (87.5%) in the MWCNT group and 0% in the C60 group and 14/18 (77.8%) in the crocidolite group (Takagi et al., 2008).

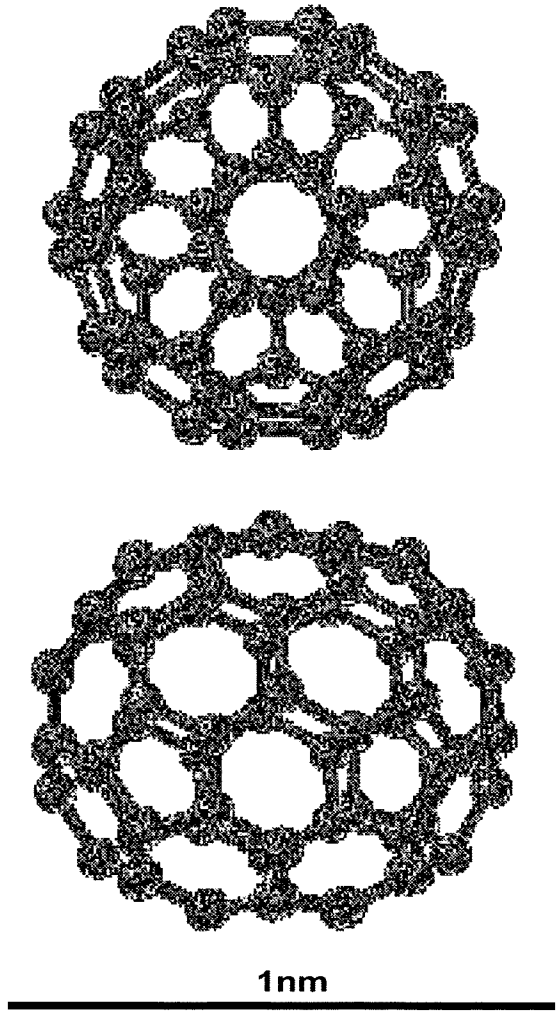


**Figure 3. Structure of Fullerene 60 (C60) and Fullerene 70 (C70).** (Courtesy of Dr. M. Ata; National Institute of Advanced Industrial Science and Technology, Japan)

c) Summary. Apparently contradictory results are reported in the rat studies. In one study, intrascrotal injection of MWCNT (approximate length 1-4 micrometers) resulted in mesothelioma in the peritoneal cavity, but intrascrotal injection of crocidolite did not induce tumor formation; in another study, mesothelioma was induced by intraperitoneal injection of crocidolite but intraperitoneal injection of MWCNT (approximate length 0.7 micrometers) did not induce tumor formation. Obviously, further studies to the confirm carcinogenic potential of MWCNT, especially MWCNT of different lengths, in rats is required. SWCNT and MWCNT induced a small amount of granulation tissue formation in the bronchioles and bronchio-alveolar area in mice. In a critically important study, MWCNT was found to induce mesothelioma in p53-/+ mice. Data pertaining to the carcinogenicity of SWCNT was negative in both rats and mice.

*3) Fullerenes (C60/70)*

Fullerene was named after Richard Buckminster Fuller, an architect who popularized the geodesic dome which resembles a spherical fullerene in appearance. C60 is composed of 60 carbons arranged at the corners of each hexagon and a bond along each edge resembling a soccer ball (Fig. 3). C70 is composed of 70 carbons (Fig. 3) and is similar in structure to C60. C60 has photocatalytic activity releasing reactive oxygen species in the presence of light.

a) Rat studies. No data is available as to carcinogenicity and related studies in rats.

b) Mouse studies. Fullerene was tested for skin tumor promotion. Female CD-1 mice were initially painted with 7,12-dimethylbenz[a]anthracene (DMBA): 20 nmol DMBA dissolved in 200 mL acetone was applied one time to shaved dorsal skin. 1 week later, a C60/C70 mixture (6:1) dissolved in benzene was applied twice a week for 25 weeks. No tumors were found in the skin. Another group of mice was treated with 12-O-tetradecanoylphorbol-13-acetate (TPA) (5mg in 200 mL acetone), a known skin tumor promoter. The incidence of tumor development in the TPA treated mice (100%) was significantly greater than in the acetone treated controls (0%). In a co-occurrent experiment ornithine decarboxylase (ODC) activity and DNA synthesis, measured by 3H-thymidine incorporation, were also increased by TPA treatment but not by C60/C70 (Nelson et al., 1993).

*c) In vitro studies related to carcinogenesis.* Fullerene C60 was treated with polyvinylpyrrolidone (PVP) and then dissolved in water. In the presence of rat liver microsomes,

treated C60 was mutagenic for Salmonella strains TA102, TA104 and YG3003, but only when exposed to visible light and not in the absence of light. Mutagenicity was reduced in the presence of antioxidants. The results suggest that singlet molecular oxygen radicals were generated by irradiating C60 with visible light. Further experiments indicated that the mutagenicity was due to oxidized phospholipids in the rat liver microsomes, in particular those present in the HPLC isolated linoleate fraction (Sera et al., 1996). Similarly, C60 induced peroxidation of lipids which caused oxidative liver cell injury in the presence of microsomes from hepatocytes (Kamat et al., 1998).

d) Summary. *In vitro*, C60 caused DNA damage when irradiated with visible light. In one *in vivo* study using mice, C60/70 did not show skin tumor promotion activity in a 26-week initiation-promotion protocol. No long-term carcinogenicity studies were reported.

## Overall Evaluation and Proposal for the Future

During the development and marketing of nanomaterials, risk assessment of these new products has been perfunctory at best. While nanomaterials have undeniable benefits, their use also has undeniable potential risk. This risk must be addressed in an unbiased and thorough manner. Only after the toxicity of the various nanomaterials is understood can their true benefits be realized.

In rodent studies, $nTiO_2$ whether administered by inhalation or intratracheal instillation was shown to induce lung tumors with characteristic squamous cell morphology in female rats. These nanomaterials did not induce lung tumors in male rats. Our own studies have also shown that instillation of $nTiO_2$ into the lungs of female rats showed tumor promoting activity and resulted in elevated ROS-mediated damage and production of inflammatory cytokines. It is reasonable to assume that other metal-derived nanoparticles, such as aluminium and copper nanoparticles, and metal containing nanoparticles, for example nCB-metal mixtures and SWCNT and MWCNT preparations, are also capable of producing these effects.

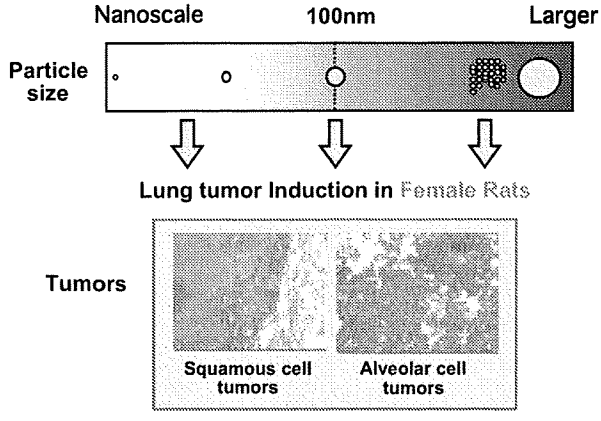


**Figure 4. Schematic Presentation of Carcinogenic Effects of $TiO_2$, Carbon Black.** Carcinogenic effects were elicited by both nano-scale and larger sized particles

Nanoparticles such as $nTiO_2$, nCB, SWCNT and MWCNT when intratracheally administered, were detected by light microscope as aggregates or agglomerates and these forms are reported to induce foreign body granulation tissue with various degree of inflammatory reaction. Although the relevance of foreign body-induced chronic inflammation to carcinogenesis is not clearly established, it is possible that reactive oxygen species (ROS) produced by macrophages attempting to destroy the foreign material in the inflammation site may cause DNA damage associated with carcinogenesis. Another possible contributing factor is metal, for example from metal-derived nanoparticles such as $TiO_2$ or from metal contaminants: these metals could also be involved in ROS production. Thus, it is possible that the observed carcinogenic effect is not specific to nanoparticles but rather associated with their ability to induce persistent foreign body-induced chronic inflammation and/or introduce metals into susceptible sites. For example, $TiO_2$ and carbon blacks larger than 100nm in diameter are known to induce lung tumors including similar squamous cell morphology (Nikula, 2000); (Pott and Roller, 2005) and both of these materials (larger than nano size) are classified as into group 2B (possibly carcinogenic to humans) by WHO/IARC.

Mechanisms for mesothelioma induction by MWCNT in mice and rats have not been elucidated yet. A possible contributing factor is metal: Transition metals, such as iron, are commonly used as a catalytic center in the formation of CNTs, and contaminating metal in SWCNT and MWCNT particles could catalyze the formation of ROS by the Fenton reaction (Liu and Okada, 1994). One example of this type of toxicity is that human keratinocytes exposed to SWCNT were killed by ROS in the media (Shvedova et al., 2003). Another possible contributing factor is the length of the MWCNT (Pott and Roller, 2005; Muller et al., 2009; Sakamoto et al., 2009).

As noted at the beginning of this review, for reliable risk assessment long-term animal studies are indispensable. This is particularly true for risk assessment of potential carcinogens. The standard for the evaluation of the carcinogenic potential of a test chemical is testing in two rodent species, generally rats and mice, of each sex, at 3 doses (0, low and high) of the test chemical for up to two years. In the studies conducted to date concerning the carcinogenic risk presented by nanoparticles, there is a noticeable lack of long term testing: No long-term tests of any type have been reported for either SWCNT or fullerenes. Importantly, the primary goal of risk assessment is not to simply ban a product from the market place, but rather to determine product safety and establish guidelines lines for its production and use and promote consumer confidence. Given the known ability of many nanomaterials to induce mechanisms which are active in humans that are risk factors for carcinogenesis, for example ROS and inflammatory cytokine production, the continued introduction of these materials into the market is alarming. Establishing the safety of these materials is urgently needed.

In this short review, available in vivo data concerning the carcinogenic effects of $nTiO_2$, nCB, SWCNT and

MWCNT, and Fullerenes is outlined. Of these, $nTiO_2$ and nCB are classified as possibly carcinogenic to humans. Testing of the carcinogenic activity of MWCNT produced mixed results. SWCNT and fullerenes have no carcinogenic activity in the studies conducted to date, however, toxicity testing of these materials has been quite limited and both of these materials have the potential to produce ROS. The observations noted here may apply to possible carcinogenic risk of other nanoparticles because of shared mechanisms of induction of inflammatory lesions and ROS generation. Our conclusions are that nanoparticles are clearly potentially toxic/carcinogenic to humans and their toxicity must be assessed, and their production and use managed appropriately.

## Acknowledgements

The authors express gratitude to Dr David B Alexander for assistance in preparation of the manuscript. The collection of the references was supported by Health and Labour Sciences Research Grant (Research on Risk of Chemical Substance 21340601, H18-kagaku-ippan-007) from the Ministry of Health, Labour and Welfare, Japan.

## References

Baan RA (2007). Carcinogenic hazards from inhaled carbon black, titanium dioxide, and talc not containing asbestos or asbestiform fibers: recent evaluations by an IARC Monographs Working Group. *Inhal Toxicol*, **19 Suppl 1**, 213-28.

Carrero-Sanchez JC, Elias AL, Mancilla R, et al (2006). Biocompatibility and toxicological studies of carbon nanotubes doped with nitrogen. *Nano Lett*, **6**, 1609-16.

Dasenbrock C, Peters L, Creutzenberg O, Heinrich U (1996). The carcinogenic potency of carbon particles with and without PAH after repeated intratracheal administration in the rat. Toxicol Lett, 88, 15-21.

Emerich DF, Thanos CG (2003). Nanotechnology and medicine. *Expert Opin Biol Ther*, **3**, 655-63.

Heinrich U, Fuhst R, Rittinghausen S, et al (1995). Chronic inhalation exposure of Wistar rats and two different strains of mice to diesel engine exhaust, carbon black, and titanium dioxide. *Inhal Toxicol*, **7**, 533-56.

Kamat JP, Devasagayam TP, Priyadarsini KI, Mohan H, Mittal JP (1998). Oxidative damage induced by the fullerene C60 on photosensitization in rat liver microsomes. *Chem Biol Interact*, **114**, 145-59.

Koyama S, Endo M, Kim YA, et al (2006). Role of systemic T-cells and histopathological aspects after subcutaneous implantation of various carbon nanotubes in mice. *Carbon*, **44**, 1079-92.

Lam CW, James JT, McCluskey R, Hunter RL (2004). Pulmonary toxicity of single-wall carbon nanotubes in mice 7 and 90 days after intratracheal instillation. Toxicol Sci, 77, 126-34.

Liu M, Okada S (1994). Induction of free radicals and tumors in the kidneys of Wistar rats by ferric ethylenediamine-N,N'-diacetate. *Carcinogenesis*, **15**, 2817-21.

Muller J, Delos M, Panin N, et al (2009). Absence of carcinogenic response to multiwall carbon nanotubes in a 2-year bioassay in the peritoneal cavity of the rat. *Toxicol Sci*, **110**, 442-8.

Muller J, Huaux F, Moreau N, et al (2005). Respiratory toxicity of multi-wall carbon nanotubes. *Toxicol Appl Pharmacol*, **207**, 221-31.

Nelson MA, Domann FE, Bowden GT, et al (1993). Effects of acute and subchronic exposure of topically applied fullerene extracts on the mouse skin. *Toxicol Ind Health*, **9**, 623-30.

Newman MD, Stotland M and Ellis JI (2009). The safety of nanosized particles in titanium dioxide- and zinc oxide-based sunscreens. *J Am Acad Dermatol*, **61**, 685-92.

Nikula KJ (2000). Rat lung tumors induced by exposure to selected poorly soluble nonfibrous particles. *Inhal Toxicol*, **12**, 97-119.

Pott F, Roller M (2005). Carcinogenicity study with nineteen granular dusts in rats. *Eur J Oncol*, **10**, 249.

Rittinghausen S, Mohr U, Dungworth DL (1997). Pulmonary cystic keratinizing squamous cell lesions of rats after inhalation/instillation of different particles. *Exp Toxicol Pathol*, **49**, 433-46.

Roco MC (2003). Nanotechnology: convergence with modern biology and medicine. *Curr Opin Biotechnol*, **14**, 337-46.

Sakamoto Y, Nakae D, Fukumori N, et al (2009). Induction of mesothelioma by a single intrascrotal administration of multi-wall carbon nanotube in intact male Fischer 344 rats. *J Toxicol Sci*, **34**, 65-76.

Sera N, Tokiwa H, Miyata N (1996). Mutagenicity of the fullerene C60-generated singlet oxygen dependent formation of lipid peroxides. *Carcinogenesis*, **17**, 2163-9.

Shvedova AA, Castranova V, Kisin ER, et al (2003). Exposure to carbon nanotube material: assessment of nanotube cytotoxicity using human keratinocyte cells. *J Toxicol Environ Health A*, **66**, 1909-26.

Takagi A, Hirose A, Nishimura T, et al (2008). Induction of mesothelioma in p53+/- mouse by intraperitoneal application of multi-wall carbon nanotube. *J Toxicol Sci*, **33**, 105-16.

Warheit DB, Laurence BR, Reed KL, et al (2004). Comparative pulmonary toxicity assessment of single-wall carbon nanotubes in rats. *Toxicol Sci*, **77**, 117-25.

Cancer Science
The official journal of the Japanese Cancer Association JCA

# Mature acinar cells are refractory to carcinoma development by targeted activation of Ras oncogene in adult rats

Hajime Tanaka,[1] Katsumi Fukamachi,[2] Mitsuru Futakuchi,[2] David B. Alexander,[2] Ne Long,[2] Shojiro Tamamushi,[4] Kohtaro Minami,[5] Susumu Seino,[5] Hirotaka Ohara,[1] Takashi Joh[1] and Hiroyuki Tsuda[2,3,6]

[1]Departments of Gastroenterology and Metabolism, [2]Molecular Toxicology and [3]Nanotoxicology Project, Nagoya City University Graduate School of Medical Sciences, Nagoya; [4]CLEA Japan Inc., Shizuoka; [5]Division of Cellular and Molecular Medicine Kobe University Graduate School of Medicine, Kobe, Japan

(Received July 20, 2009/Revised October 8, 2009/Accepted October 13, 2009/Online publication November 16, 2009)

**Pancreatic ductal adenocarcinoma (PDA) is one of the most debilitating malignancies in humans. A thorough understanding of the cytogenesis of this disease will aid in establishing successful treatments. We have developed an animal model which uses adult Hras$^{G12V}$ and Kras$^{G12V}$ transgenic rats in which oncogene expression is regulated by the Cre/loxP system and neoplastic lesions are induced by injection of adenovirus-expressing Cre recombinase. When adenovirus with Cre recombinase under the control of the CMV enhancer/chicken β-actin (CAG) promoter (Ad-CAG-Cre) is injected into the pancreatic duct of these animals, pancreatic neoplasias develop. Pathologically, the origin of these lesions is duct, intercalated duct, and centroacinar cells, but not acinar cells. The present study was undertaken to test the effect of acinar cell-specific oncogenic *ras* expression. Adult transgenic rats were injected with adenovirus with Cre recombinase under the control of the acinar cell-specific promoters amylase (Ad-Amy-Cre) and elastase-1 (Ad-Ela-Cre) or under the control of the non-specific CAG promoter. Injection of either Ad-Amy-Cre or Ad-Ela-Cre into the pancreatic ducts of transgenic animals in which oncogenic *Kras* is tagged with hemagglutinin (HA), HA-Kras$^{G12V}$ rats resulted in expression of oncogenic *ras* in acinar cells but not in duct, intercalated duct, or centroacinar cells. Notably, injected animals did not develop any observable proliferative or neoplastic lesions. In marked contrast, injection of Ad-CAG-Cre resulted in pancreatic cancer development within 4 weeks. These results indicate that adult acinar cells are refractory to Ras oncogene activation and do not develop neoplasia in this model. (*Cancer Sci* 2010; 101: 341–346)**

Pancreatic ductal adenocarcinoma (PDA) is a highly lethal disease, which is usually diagnosed in an advanced state. Most patients die within 1 year of diagnosis, [1] and the 5-year survival rate is <5%.[2] Understanding of the cytogenesis of PDA offers new directions for targeted therapeutic approaches to combat this disease.

Previously, we reported on an animal model in which pancreatic neoplasia was induced in adult Hras$^{G12V}$ transgenic rats by injection of adenovirus with Cre recombinase under the control of the CMV enhancer/chicken β-actin (CAG) promoter into the pancreatic duct.[3] In these animals, it was shown that duct, intercalated duct, centroacinar, and acinar cells were all infected with the adenovirus, but induced pre-neoplastic and neoplastic lesions were shown to express only duct cell-specific characteristics and not acinar cell-specific characteristics. Moreover, proliferative lesions were not observed in acinar cells. Therefore, we hypothesized that PDA does not develop from adult pancreatic acinar cells in this model.

The present study was undertaken to directly test the capability of mature acinar cells to develop into a neoplastic lesion. Transgenic rats with an Hras or hemagglutinin (HA)-tagged Kras oncogene were injected with Cre recombinase expressing adenoviruses in which Cre expression was under the control of promoters specifically active in acinar cells. Mature acinar cells in injected rats did express active Ras proteins, but did not develop any proliferative or neoplastic lesions.

## Materials and Methods

**Generation of transgenic rats.** For the generation of transgenic rats conditionally expressing human Kras$^{G12V}$, we first made a cDNA fragment encoding the human Kras4B$^{G12V}$ with a 3× HA tag sequence at its 5′ end (HA-Kras$^{G12V}$). The HA-Kras$^{G12V}$ cDNA was subcloned into the SacI/KpnI site of pCALNL5 (DNA Bank, RIKEN Bio Resource Center, Ibaraki, Japan)[4,5] to produce pCALNLHAKras. pCALNLHAKras was digested with SalI/HindIII. The purified cassette (Fig. 1A) was injected into the pronuclei of Sprague–Dawley rats (CLEA Japan, Tokyo, Japan). Techniques used for the generation of transgenic rats were the same as those reported previously.[3,6] A total of 265 injected eggs were transplanted into pseudo-pregnant Sprague–Dawley rats. Of 37 potential transgenic rats screened, four male and one female rat were shown by PCR to carry the transgene. Transgenic founder rats were mated with Sprague–Dawley rats, and offspring were screened for the presence of the transgene by PCR analysis of genomic DNA isolated from tail biopsies at the age of 3 weeks. The following primers were used: 5′-TCTGGATCAAATCCGAACGC-3′, 5′-TGACCTGCTGTGTC-GAGAAT-3′. Two founder rats carrying a CALNLHAKras$^{G12V}$ transgene transmittable to descendent generations (Kras301and Kras327) and two founder rats (Kras409 and Kras417) carrying a non-tagged Kras$^{G12V}$ transgene were established using the same cassette (data not shown). In this study, we used Kras301 and Kras327. Hras250 rats conditionally expressing human Hras$^{G12V}$ were generated as previously described. [3] They were maintained in plastic cages in an air-conditioned room with a 12-h light/12-h dark cycle. All experiments were conducted according to the Guidelines for Animal Experiments of the Nagoya City University Graduate School of Medical Sciences.

**Preparation of adenovirus vectors.** Adenoviruses in which either the mouse amylase-2 or the rat elastase-1 promoter drove the expression of Cre recombinase (Ad-Amy-Cre or Ad-Ela-Cre) (Fig. 1B) were prepared as described previously.[7] Recombinant adenovirus vectors carrying the *Cre* gene (Ad-CAG-Cre) (Fig. 1B) and empty adenovirus vector were prepared as described previously.[3] Recombinant adenovirus vectors were amplified in HEK-293 cells and then purified using Vivapure

[6]To whom correspondence should be addressed.
E-mail: htsuda@med.nagoya-cu.ac.jp

doi: 10.1111/j.1349-7006.2009.01410.x

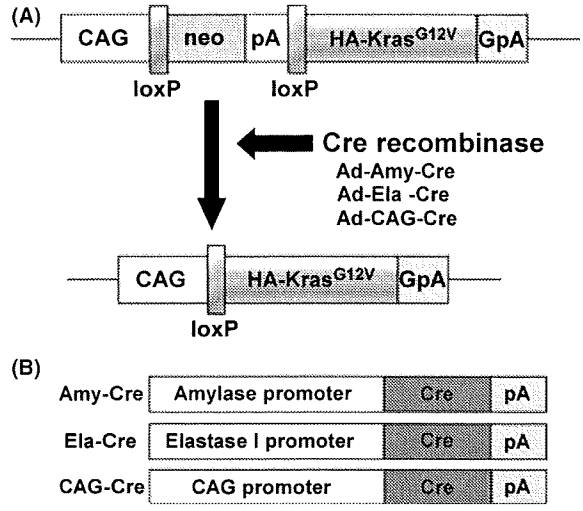


**Fig. 1.** Conditional expression of Kras$^{G12V}$ transgene. (A) The CALNL-HAKras$^{G12V}$ transgene is comprised of a hybrid CMV enhancer/chicken β-actin (CAG) promoter, a cassette for the neomycin resistance gene flanked by loxP sites, and a sequence containing a human Kras$^{G12V}$ with a hemagglutinin (HA)-tag. Infection with the Cre recombinase-expressing adenovirus results in Cre-mediated recombination of the transgene and removal of the neo-coding region and its associated mRNA polyadenylation signal, generating a functional HA-Kras$^{G12V}$ gene expression unit. GpA, rabbit- β-globin poly(A) site; pA, SV40 early poly(A) site. (B) Cre recombinase with nuclear localization signal expressing adenovirus in which Cre expression is under the control of three different promoters: the amylase promoter and the elastase-1 promoter which are active in acinar cells, and the CAG promoter which is a nonspecific promoter.

Adenopack (Vivascience, Hannover, Germany). The titer of the adenovirus was determined by using the Rapid titer kit (Clontech, Mountain View, CA, USA). The virus stock was concentrated to $1.0 \times 10^{10}$ pfu/mL.

**Induction of active Ras in the pancreas.** Adenovirus vectors were injected into the pancreatic ducts of 12-week-old adult male rats through the common duct as previously reported. To induce active Ras specifically in acinar cells, adenoviruses ($6 \times 10^8$ pfu/rat) in which the expression of Cre recombinase was under the control of acinar cell specific promoters, either the amylase-2 (Ad-Amy-Cre) or elastase-1 (Ad-Ela-Cre) promoter, were used. To induce active Ras non-specifically, adenoviruses ($6 \times 10^8$ pfu/rat) in which the expression of Cre recombinase was under the control of the non-specific CAG promoter were used.

**Western blotting.** Western blot analysis and detection of activated Ras protein was performed using a Ras Activation Assay kit (Upstate, Lake Placid, NY, USA) as described previously.[3,8] Concentrations of the proteins were determined by Bio-Rad Protein assay. Proteins were separated by SDS-PAGE. After transfer to a polyviniliden defluoride membrane, the membrane was blocked with 5% nonfat milk and then incubated for 1 h at room temperature with primary antibodies. The following antibodies were used: anti-Ras, clone Ras10 (Upstate) diluted 1:4000; HA-probe (Y-11; Santa Cruz Biotechnology, Santa Cruz, CA, USA) diluted 1:1,000; and monoclonal anti-β-actin (A5441; Sigma, St Louis, MO) diluted 1:10 000. The primary antibodies were detected using HRP-conjugated secondary antibodies (Southern Biotechnology Associates, Birmingham, AL, USA) and ECL plus (GE Heallthcare UK, Buckinghamshire, UK).

**Immunostaining.** Tissues were fixed in 10% formalin or 4% paraformaldehyde fixative and embedded in paraffin. For Ki67, proliferating cell nuclear antigen (PCNA), and HA-tag staining, sections were boiled for 10 min in a 10-mM citrate buffer (pH 6.0) and then allowed to cool in PBS for 30 min before incubation with antibodies. For anti-α-amylase staining, section slides were incubated for 10 min in a 0.1% trypsin solution at 37°C and then washed in PBS for 5 min before incubation with antibodies.

Before staining, each section was blocked with 10% goat serum (Nichirei Bio Science, Tokyo, Japan) for 5 min at room temperature. The slides were incubated overnight at 4°C with primary antibodies against Ki67antigen (NCL-Ki67-p; Novocastra Laboratories, Newcastle, UK), diluted 1:3000; PCNA (clone PC10; DakoCytomation, Glostrup, Denmark), diluted 1:50; HA-Tag (6E2; Cell Signaling, Danvers, MA, USA), diluted 1:100; or anti-α-amylase (A8273; Sigma, St Louis, MO, USA), diluted 1:200. Slides were incubated with secondary antibodies conjugated with Alexa Fluor488, 546, and 647 (Invitrogen, Carlsbad, CA, USA), and images were obtained with a FLUOVIEW FV300 confocal microscope (Olympus, Tokyo, Japan) or a BZ-9000 fluorescence microscope (Keyence, Osaka, Japan).

## Results

**Targeted activation of HA-Kras$^{G12V}$ transgenes in mature acinar cells.** Injection of transgenic rats with Cre recombinase expressing adenovirus resulted in excision of the stuffer DNA between the CAG promoter and the transgene and consequent expression of the transgene in infected cells (Fig. 1A). Kras301/ 327 rats were injected with Ad-Amy-Cre or Ad-Ela-Cre. Expression of HA-Kras$^{G12V}$ was observed only in amylase-positive acinar cells and not in duct, centroacinar, intercalated duct, or islet cells (Table 2) (Fig. 2A; data for Ad-Ela-Cre is identical to that of Ad-Amy-Cre). Some acinar cells with nuclei with an "owl-eye" or "ground glass" appearance, which are generally used for identification of virus-infected cells,[9] in rats treated with Ad-Amy-Cre or Ela-Cre were also positive for both amylase and HA (Fig. 2A-d,e). All acinar cells positive for HA were entirely negative for Ki67 (Fig. 2A).

**Lack of PDA development by targeted activation of Ras$^{G12V}$ in mature acinar cells.** None of the Kras301/327 rats injected with Ad-Amy-Cre or Ela-Cre developed pancreatic lesions (Ad-Amy-Cre, 0 out of 5; Ad-Ela-Cre, 0 out of 7) after 8 weeks (Fig. 2B, Table 1). Similarly, none of the Hras250 rats injected with Ad-Amy-Cre or Ad-Ela-Cre ($6 \times 10^8$ pfu/rat) developed pancreatic lesions (Ad-Amy-Cre, 0 out of 7; Ad-Ela-Cre, 0 out of 8) after 8 weeks (Table 1). In addition, Kras301/327 rats injected with higher titers of Ad-Amy-Cre ($6 \times 10^9$ pfu/rat) did not develop pancreatic lesions (data not shown). Finally, tumor induction was not observed in injected Kras301/327 rats even after 6 months (data not shown).

**Neoplasia development by activation of Ras$^{G12V}$ transgenes in ductular cells.** Both Kras301/327 and Hras250 rats injected with Ad-CAG-Cre ($6 \times 10^8$ pfu/rat) developed pancreatic neoplasias: 22 of 22 Kras301/327 rats and 30 of 35 and Hras250 rats after 2 to 4 weeks (Table 1), as observed in our previous report.[3] Pancreatic neoplasias were also observed in Kras301/327 rats injected with lower titers of Ad-CAG-Cre ($6 \times 10^7$ pfu/rat) (data not shown). Activation of the transgene in the pancreatic ductal lesions of Kras301/327 rats was shown by Western blotting using anti-HA antibody (Fig. 3). The expression of HA-Kras$^{G12V}$ was detected in pancreatic intraepithelial neoplasia (PanIN) and neoplastic lesions, but not in normal-looking pancreatic duct cells or stromal cells (Fig. 4A). Ki67 or PCNA and HA were positive in PanIN lesions (Fig. 4B) and in many neoplastic cells (Fig. 4C).

## Discussion

The morphological and molecular signatures associated with human pancreas tumors suggests that duct epithelium is



doi: 10.1111/j.1349-7006.2009.01410.x

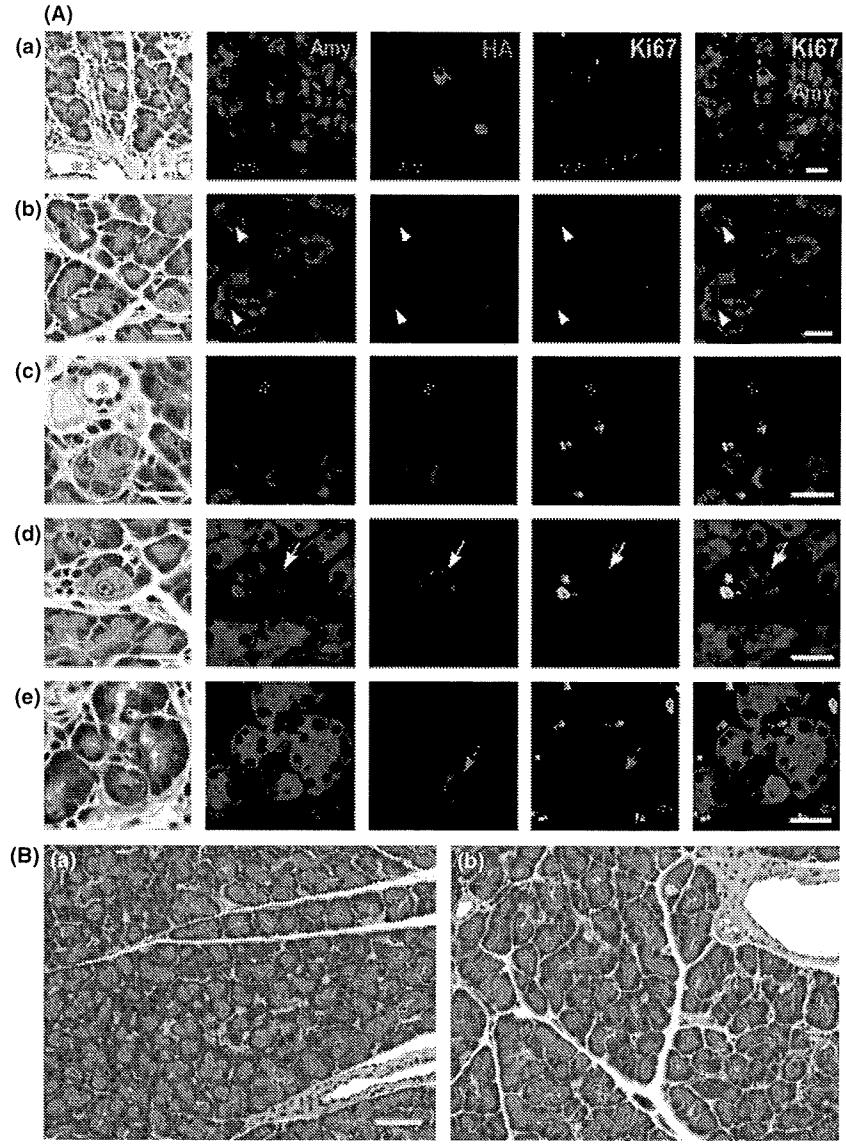


**Fig. 2.** Acinar cell-specific expression of hemagglutinin (HA)-Kras$^{G12V}$. (A) Localization of amylase (blue) protein, HA-Kras$^{G12V}$ (red) and Ki67 (green) at 2 days after injection of virus with Ad-Amy-Cre (a, b, c, d) and Ela-Cre (e). All the HA-Kras$^{G12V}$ positive cells (red) were acinar cells; expression was not observed in duct cells (**), centroacinar cells (yellow arrowhead), or small duct cells (*). Most virally infected acinar cells positive for HA-Kras$^{G12V}$ were indistinguishable from non-infected acinar cells by hematoxylin–eosin staining. Some infected acinar cells have nuclei with a so-called "owl-eye" (yellow arrows) or "ground glass" (red arrows) appearance. Ki67 (green) is not present in the nuclei of the cells expressing HA-Kras$^{G12V}$ (red). Bar, 20 μm. (B) None of the Ad-Amy-Cre (a) or the Ad-Ela-Cre (b) groups displayed any pancreatic lesions, even after 8 weeks. Bar, 50 μm.

responsible for the development of PDA, but it remains unclear whether other pancreatic cells might also contribute to the cytogenesis of these lesions. In our previous study using the Hras250 rat, 4 weeks after injection of adenovirus with Cre recombinase under the control of the constitutive CAG promoter, proliferative lesions in the duct epithelium, intercalated ducts, and centroacinar cells were widespread, but we could not detect any proliferative lesions in acinar cells; moreover, subsequent neoplastic lesions expressed only duct cell-specific characteristics and not acinar cell-specific ones.[3] We have obtained essentially identical results with Kras transgenic rats as we did with Hras250 rats (data not shown). These results suggest that PDAs may arise from centroacinar cells, intercalated duct, or pancreatic duct epithelium, but not from acinar cells.

The current study was undertaken to clarify whether mature acinar cells in adult rats could be induced to develop to PDA by targeted activation of oncogenic *ras*. Activation of oncogenic *ras* in acinar cells did not lead to the development of any observable pancreatic lesions, while nonspecific activation of oncogenic *ras* in the pancreas resulted in rapid development of

**Table 1. Pancreas tumor induction by activation of Hras$^{G12V}$ or hemagglutinin (HA)-Kras$^{G12V}$ oncogene after Cre-adenovirus injection**

| Oncogene | Virus vector | Number of rats with tumor (%) |
|---|---|---|
| Hras$^{G12V}$ | Amylase-Cre | 0/7 (0) |
| | Elastase-Cre | 0/8 (0) |
| | CAG-Cre | 30/35 (87.5) |
| HA-Kras$^{G12V}$ | Amylase-Cre | 0/5 (0) |
| | Elastase-Cre | 0/7 (0) |
| | CAG-Cre | 22/22 (100) |

**Table 2. Target cell and tumor type in Hras$^{G12V}$ and hemagglutinin (HA)-Kras$^{G12V}$transgenic rats**

| Virus vector | Target cells | | | Tumor yield | |
|---|---|---|---|---|---|
| | Acinar cells | Centroacinar cells | Duct cells | Acinar cells | Duct cells |
| Amy-Cre | + | – | – | – | – |
| Ela-Cre | + | – | – | – | – |
| CAG-Cre[3] | + | + | + | – | + |

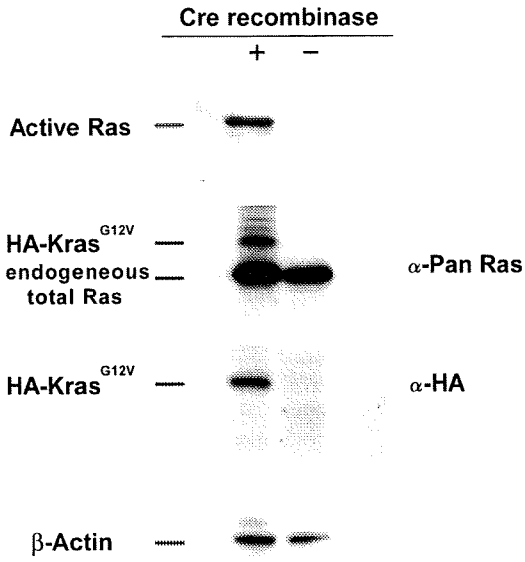


**Fig. 3.** Transgene activation in Kras301 and 327 by Western blotting. A high level of active Ras and hemagglutinin (HA)-Kras$^{G12V}$ were detected in the pancreas of the Ad-CAG-Cre-treated rats. The amount of active Ras was analyzed by RBD (Ras-binding domain of Raf-1) pull-down assay followed by Western blotting with anti-pan Ras antibody. HA-Kras$^{G12V}$ and endogeneous total Ras was detected using anti-Pan Ras antibody. HA-Kras$^{G12V}$ was detected using anti-HA antibody. β-Actin was used as a loading control.

pancreatic neoplasias. Our results clearly show that conditional expression of oncogenic *ras* in acinar cells in fully developed pancreas tissue does not result in induction of neoplasia in this model (Table 1).

Previous reports in which Kras was activated in immature acinar cells during embryonic development[10,11] suggested that acinar-ductal metaplasia played a role in the development of PDA. In these models, premalignant acinar-ductal metaplasia and acinar tumor mixed with duct-like lesions developed in transgenic mice. This acinar-ductal metaplasia, however, may have occurred before the pancreas fully developed. Our model, on the other hand, targets mature acinar cells which express digestive enzymes, amylase and/or elastase, and these cells do not undergo acinar-ductal metaplasia in response to ras activation.

Our results are in agreement with a recent study in which the distribution of *K-RAS2* gene mutations was extensively examined in surgically resected pancreata from human patients and which concluded that ductal neoplasms of the human pancreas did not appear to arise from acinar cells.[12]

Kras mutations were not observed in pancreatic acinar cell carcinoma (ACC) induced in mature rats by administration of azaserine.[13] Furthermore, alterations in the APC/β-catenin pathway were detected in 23.5% of human ACC,[14] but mutation of Kras was not observed.[15,16] Thus, it is possible that APC/β-catenin or another pathway, but not necessarily Kras activation, is involved in ACC development.

While pancreas cancer in the hamster model is also believed to arise from ductal epithelial hyperplasia,[17,18] several studies using transgenic mice[11,19–24] suggest that PDA may develop from acinar cells. In most of these studies, however, oncogenic stimuli are present during embryonic development, prior to the development of a mature pancreas. Therefore, the acinar cells which were activated and developed into neoplasias in these models could very well be at a different developmental stage to the acinar cells which are present in a mature pancreas. This is important because the majority of PDA patients are 60 years of age or older. It is highly unlikely that an oncogenic insult occurring in the uterus is the root cause of most of these PDAs. Moreover, epidemiological studies indicate the incidence of PDA is closely related to lifestyle.[25] Therefore, PDA most likely develops from cells in the mature pancreas. Consequently, pancreas tumor models in which the oncogenic insult occurs during embryonic development are unlikely to be appropriate for determining the cytogenesis of human PDA.

Two models[22–24] use conditional activation of Cre recombinase to active oncogenic *ras* in adult animals: one model[22] uses the tet-off system to control expression of Cre recombinase and the other model[23,24] uses the tamoxifen-estrogen receptor system to control nuclear localization of Cre recombinase. These studies had slightly conflicting results. In one study, expression of oncogenic *ras* in adult acinar cells did not by itself induce pancreatic lesions; additional treatment causing chronic pancreatitis was also needed.[22] In the other study, expression of oncogenic *ras* was sufficient to induce PanIN-like lesions.[23,24] In our model, we clearly showed that while expression of oncogenic *ras* is sufficient to induce duct, intercalated duct, and/or centroacinar cells to develop into pancreatic cancers, it is not sufficient to induce acinar cells to develop into pancreatic cancers. Whether these discrepancies are due to experimental procedures, the nature of the Cre recombinase constructs used, or differences between mice and rats remains to be resolved. There are however, a few readily apparent differences. In our rat system, there is no expression of Cre recombinase in the animal until injection of adenovirus-expressing Cre recombinase, and the expression of Cre recombinase is transient. In the model which uses tamoxifen, on the other hand, Cre recombinase is expressed during embryonic development, but nuclear localization is regulated by tamoxifen.[23,24] In this model, however, there was a low level of tamoxifen-independent recombination events resulting in expression of oncogenic *ras* in embryonic acinar cells.[24] It is possible that embryonic acinar cells expressing oncogenic *ras* did not fully differentiate in the adult pancreas; for example, in the mouse colon expression of Kras$^{G12V}$ inhibits differentiation.[26] Therefore, it is possible that in the tamoxifen-estrogen regulated model,[23,24] the acinar cells which were activated to undergo metaplasia to duct-like cells in the adult were not actually mature acinar cells. The other obvious difference is that in the model regulated by the tet-off system, two events were required to induce pancreas cancer: activation of oncogenic *Kras* and chronic pancreatitis.[22] Chronic pancreatitis would very likely result in the death of mature acinar cells and their replacement from a proliferative compartment. It is possible that these replacement cells are not fully mature acinar cells, again suggesting the possibility that the acinar cells which underwent metaplasia to duct-like cells were not actually mature acinar cells.

The primary aim of this study was to determine whether activation of oncogenic Kras in mature, digestive enzyme-secreting acinar cells would lead to pancreatic lesions. Our findings support our earlier hypothesis that PDA does not develop from Kras activation in mature acinar cells. It is possible, however, that PDA could develop from Kras activation in immature acinar cells, and in this regard we would like to emphasize the results of Guerra *et al.*[22] in which activation of Kras in the mature pancreas accompanied by chronic pancreatitis resulted in induction of PDA in transgenic mice. Importantly, chronic pancreatitis has been shown to be one of the main risk factors for PDA development in humans.[27,28]

Other factors which may influence PDA development in our model are inflammation and fibrosis. Shortly after infection of pancreatic tissue with Cre recombinase carrying adenovirus to activate the Kras transgene, infiltration of macrophages and lymphocytes could be observed. This infiltration is presumably in response to viral infection. A moderate degree of inflammation, however, was still observed in the stromal tissue surrounding the tumors when PDA developed. These finding suggest that



doi: 10.1111/j.1349-7006.2009.01410.x